Read HM, Mills G, Johnson S, Tsai P, Dalton J, Barquist L, Print CG, Patrick WM, Wiles S. 2016. The *in vitro* and *in vivo* effects of constitutive light expression on a bioluminescent strain of the mouse enteropathogen *Citrobacter rodentium*. PeerJ 4:e2130 https://doi.org/10.7717/peerj.2130

The *in vitro* and *in vivo* effects of constitutive light expression on the mouse enteropathogen *Citrobacter rodentium*

Hannah M Read, Grant Mills, Sarah Johnson, Peter Tsai, James Dalton, Lars Barquist, Cristin G Print, Wayne M Patrick, Siouxsie Wiles

Bioluminescent reporter genes, such as those from fireflies and bacteria, let researchers use light production as a non-invasive and non-destructive surrogate measure of microbial numbers in a wide variety of environments. As bioluminescence needs microbial metabolites, tagging microorganisms with luciferases means only live metabolically active cells are detected. Despite the wide use of bioluminescent reporter genes, very little is known about the impact of continuous (also called constitutive) light expression on tagged bacteria. We have previously made a bioluminescent strain of *Citrobacter rodentium*, a bacterium which infects laboratory mice in a similar way to how enteropathogenic *Escherichia coli* (EPEC) and enterohaemorrhagic *E. coli* (EHEC) infect humans. In this study, we investigated whether constitutive light expression makes the bioluminescent *C. rodentium* strain ICC180 less competitive when competed against its non-bioluminescent parent (strain ICC169). To understand more about the metabolic burden of expressing light, we also compared the growth profiles of the two strains under approximately 2000 different conditions. We found that constitutive light expression in ICC180 was near-neutral in almost every non-toxic environment tested. However, we also found that the non-bioluminescent parent strain has a competitive advantage over ICC180 during infection of adult mice, although this was not enough for ICC180 to be completely outcompeted. In conclusion, our data suggests that constitutive light expression is not metabolically costly to *C. rodentium* and supports the view that bioluminescent versions of microbes can be used as a substitute for their non-bioluminescent parents to study bacterial behaviour in a wide variety of environments.

PeerJ Preprints | https://doi.org/10.7287/peerj.preprints.1993v1 | CC-BY 4.0 Open Access | rec: 23 Apr 2016, publ: 23 Apr 2016

The *in vitro* and *in vivo* effects of constitutive light expression on the mouse enteropathogen *Citrobacter rodentium*.

Read H,[1,2] Mills G,[1,2] Johnson S,[1,2] Tsai P,[3] Dalton J,[1,2,4] Barquist L,[5] Print C,[2,3,4] Patrick WM,[4,6] Wiles S.[1,2,4*]

[1]Bioluminescent Superbugs Lab, [2]Department of Molecular Medicine and Pathology, University of Auckland, Auckland, New Zealand; [3]Bioinformatics Institute, School of Biological Sciences, University of Auckland, New Zealand; [4]Maurice Wilkins Centre for Molecular Biodiscovery, New Zealand; [5]Institute for Molecular Infection Biology, University of Würzburg, Würzburg, Germany; [6]Department of Biochemistry, University of Otago, Dunedin, New Zealand.

*Corresponding author: Dr. S Wiles
Mailing address: Dept. Molecular Medicine and Pathology, University of Auckland, Private Bag 92019, Auckland, New Zealand.
Tel: +64 9 3737599 Extension 84284
Fax: +64 9 3738784
E-mail: s.wiles@auckland.ac.nz

Running title: Bioluminescent *Citrobacter rodentium*: the minimal price of light.

Key words: *Citrobacter rodentium*; EPEC; EHEC; bioluminescence; lux; luciferase; fitness costs; mouse model; biophotonic imaging; phenotypic microarray.

Abstract

Bioluminescent reporter genes, such as those from fireflies and bacteria, let researchers use light production as a non-invasive and non-destructive surrogate measure of microbial numbers in a wide variety of environments. As bioluminescence needs microbial metabolites, tagging microorganisms with luciferases means only live metabolically active cells are detected. Despite the wide use of bioluminescent reporter genes, very little is known about the impact of continuous (also called constitutive) light expression on tagged bacteria. We have previously made a bioluminescent strain of *Citrobacter rodentium*, a bacterium which infects laboratory mice in a similar way to how enteropathogenic *Escherichia coli* (EPEC) and enterohaemorrhagic *E. coli* (EHEC) infect humans. In this study, we investigated whether constitutive light expression makes the bioluminescent *C. rodentium* strain ICC180 less competitive when competed against its non-bioluminescent parent (strain ICC169). To understand more about the metabolic burden of expressing light, we also compared the growth profiles of the two strains under approximately 2000 different conditions. We found that constitutive light expression in ICC180 was near-neutral in almost every non-toxic environment tested. However, we also found that the non-bioluminescent parent strain has a competitive advantage over ICC180 during infection of adult mice, although this was not enough for ICC180 to be completely outcompeted. In conclusion, our data suggests that constitutive light expression is not metabolically costly to *C. rodentium* and supports the view that bioluminescent versions of microbes can be used as a substitute for their non-bioluminescent parents to study bacterial behaviour in a wide variety of environments.

Introduction

Bioluminescence is the by-product of a chemical reaction which has evolved in a wide variety of creatures for different purposes. This 'living light' allows fireflies like *Photinus pyralis* to find a mate[1], larvae like the New Zealand glow worm *Arachnocampa luminosa* to lure prey[2], and the bacterium *Aliivibrio fischeri* (formally *Vibrio fischeri*) to camouflage its nocturnal symbiont, the Hawaiian bobtail squid, while hunting[3]. Bioluminescence is produced by the oxidation of a substrate (a luciferin) by an enzyme (a luciferase), which usually requires energy and oxygen. Cloning of the bioluminescence genes from *P. pyralis*[4], *V. fischeri*[5] and *Photorhabdus luminescens*[6], has let researchers use light production as a real-time non-invasive and non-destructive surrogate measure of microbial numbers in a wide variety of different culture environments, including within laboratory animals[7]. This has proven particularly useful for studying microorganisms which take several weeks to grow on selective media, such as the bacterium *Mycobacterium tuberculosis*[8,9]. As bioluminescence requires microbial metabolites, such as ATP and reduced flavin mononucleotide ($FMNH_2$), tagging microorganisms with luciferases means only live, metabolically active cells are detected.

Of the available bioluminescent reporter systems, the most widely used in bacteriology research is the bacterial luminescence reaction, encoded by the *lux* gene operon. The reaction involves the oxidation of a long chain aldehyde and $FMNH_2$, resulting in the production of oxidised flavin (FMN), a long chain fatty acid, and the emission of light at 490 nm [10]. The reaction is catalysed by bacterial luciferase, a 77 kDa enzyme made up of an alpha and a beta subunit encoded by the *luxA* and *luxB* genes, respectively. The *luxC*, *D* and *E* genes encode the subunits of a multi-enzyme complex responsible for regenerating the aldehyde substrate from the fatty acid produced by the reaction. A significant advantage of the bacterial bioluminescence system is the ability to express the biosynthetic enzymes for substrate synthesis, allowing light to be

produced constitutively. One of the underlying motivations for using *lux*-tagged bacteria is the reduction in the number of animals needed for *in vivo* experiments, a legislative requirement in many countries. Using a technique known as biophotonic imaging, tagged bacteria can be non-invasively and non-destructively visualised and quantified on multiple occasions from within the same group of infected animals, whereas culture based techniques need groups of animals to be euthanised at each time point of interest[7]. However, very little is known about the impact of constitutive light expression on tagged bacteria. We hypothesise that light production will impose a metabolic burden on the tagged bacteria, with the actual fitness costs dependent on the host bacterial species, the site of insertion of the bioluminescence genes and their expression levels.

We have previously made a *lux*-tagged derivative of *Citrobacter rodentium*[11], a bacterium that infects laboratory mice using the same virulence mechanisms as the life-threatening pathogens, enteropathogenic *Escherichia coli* (EPEC) and enterohaemorrhagic *E. coli* (EHEC) use to infect humans[12,13]. *C. rodentium* ICC180 contains a single chromosomally-located copy of the *lux* operon from P. *luminescens*, alongside a gene for resistance to the antibiotic kanamycin. We have previously non-invasively tracked ICC180 during infection of mice[14], demonstrating that *C. rodentium* rapidly spreads between infected and uninfected animals and that bacteria shed from infected mice are 1,000 times more infectious than laboratory grown bacteria[15]. While we have shown that ICC180 can reach similar numbers within the gastro-intestinal tracts of infected mice when compared to its non-bioluminescent parent strain ICC169[11], we have never fully investigated the impact of constitutive light expression on the fitness of ICC180.

In this study we set out to determine whether constitutive expression of the *lux* operon provides a competitive disadvantage for *C. rodentium* ICC180 when competed against its non-bioluminescent parent ICC169 in a range of in vitro and in vivo environments. We also

sequenced the genome and associated plasmids of ICC180 to determine whether there were any other genetic differences between the two strains, perhaps as a result of the transposon mutagenesis technique[16] used to generate ICC180. Finally, we compared the growth profiles of the two strains using the BIOLOG Phenotypic Microarray (PM) system, a rapid 96-well microtitre plate assay for phenotypically profiling microorganisms based on their growth under approximately 2000 different metabolic conditions[17].

Materials and methods

Bacterial strains and culture conditions. The bacterial strains used in this study were *Citrobacter rodentium* ICC169 (spontaneous nalidixic acid resistant mutant)[11] and ICC180 (nalidixic acid and kanamycin resistant)[11]. Bacteria were revived and grown from frozen stocks stored at -80°C in order to prevent adaptation of *C. rodentium* over multiple laboratory subcultures. Bacteria were grown at 37°C with shaking at 200 revolutions per minute (RPM) in LB-Lennox media (Fort Richard Laboratories Ltd., Auckland, New Zealand) or in defined minimal media (modified Davis & Mingioli media[18]), containing ammonium sulphate [1 g l^{-1}], potassium dihydrogen phosphate [4.5 g l^{-1}], dipotassium hydrogen phosphate anhydrous [10.5 g l^{-1}], sodium citrate dihydrate [5 g l^{-1}], magnesium sulfate heptahydrate [24.65 mg l^{-1}], thiamine [0.5 mg l^{-1}], supplemented with 1% glucose) at 37°C. Antibiotics (kanamycin [50 ug ml^{-1}], nalidixic acid [50 ug ml^{-1}]) were only added to the media if they were required for selection. All chemicals and antibiotics were obtained from Sigma-Aldrich (Australia).

Genome sequencing and analysis. Genomic DNA was prepared from bacteria grown overnight in LB-Lennox broth. Whole genome sequencing was performed using the Illumina HiSeq platform by BGI (Hong Kong). A total of 3,414,820 paired-end 90 bp reads were generated for ICC169 and 3,369,194 for ICC180. Data was quality trimmed using DynamicTrim[19] (minimum Phred score 25) and filtering of reads shorter than 45 bp after quality trimming was performed using LengthSort[19]; both programmes are part of the SolexaQA software package[19]. After filtering, 2,444,336 paired reads were retained for ICC169 and 2,383,491 for ICC180. All remaining high quality and properly paired reads were mapped to the reference strain *C. rodentium* ICC168 (Genbank accession number FN543502.1[20]) using the default settings in BWA[21]. On average, 95% of all high quality reads mapped uniquely to ICC168 (94.8% for ICC169 and 95.2% for ICC180) and single nucleotide polymorphisms (SNPs) and indels that were present only in ICC180 at 100% were identified using Samtools

mpileup[22]. SNPs and indels were confirmed by PCR and sequencing. In addition, the reads were also analysed using BreSeq version 0.24rc6[23], which identified predicted mutations that were statistically valid. To locate the insertion site of the lux operon and kanamycin resistance (Km^R) gene, we first performed de novo assembly on quality trimmed data for ICC180 data using EDENA v3.0[24]. All assembled contigs were mapped to the *C. rodentium* reference strain ICC168 using Geneious[25] and contigs unmapped to ICC168 were BLAST searched against the *lux* operon and Km^R gene. We located both the *lux* operon and Km^R gene on an unmapped contig 117,921 bp long. To identify the position of this contig, we broke the contig into two segments based on the location of *lux* operon and Km^R gene positions on the contig, and performed additional reference mapping to ICC168 to identify the insertion site. To determine changes to the plasmids present in *C. rodentium*, reads were also mapped to the sequenced plasmids pCROD1 (Genbank accession number FN543503.1), pCROD2 (Genbank accession number FN543504.1), pCROD3 (Genbank accession number FN543505.1), and pCRP3 (Genbank accession number NC_003114).

Phenotypic microarrays. Phenotypic microarrays were performed by BIOLOG Inc. (California, USA) as described previously[17]. Assays were performed in duplicate using plates PM1-20 (Supplementary Table 1). The data was exported and analysed in the software package R as previously described[26]. Briefly, growth curves were transformed into Signal Values (SVs)[27] summarising the growth over time while correcting for background signal. PCA showed a clear separation by genotype, suggesting reproducible differences in metabolism between the two strains. A histogram of log signal values displayed a clear bimodal distribution, which we interpreted as representing non-respiring cells ('off', low SV) and respiring cells ('on', high SV), respectively. Normal distributions were fitted to these two distributions using the R MASS package, and these models were then used to compute log-odds ratios for each well describing the probability that each observation originated from the 'on' or 'off' distribution. Wells which

were at least 4 times more likely to come from the 'on' distribution than the 'off' in both replicates were considered to be actively respiring. In order to determine the significance of observed differences between genotypes, we applied the moderated t-test implemented in the limma R/Bioconductor package[28]. Wells with a Benjamini-Hochberg corrected P-value of less than 0.05, that is allowing for a false discovery rate of 5%, and which were called as actively respiring for at least one genotype, were retained for further analysis. The data was also analysed using the DuctApe software suite[29]. Growth curves were analysed using the dphenome module, with the background signal subtracted from each well. Based on the results of an elbow test (Supplementary Fig.1), 7 clusters were chosen for k-means clustering. An Activity Index (AV) was created based on the clustering, ranging from 0 (minimal activity) to 6 (maximal activity). AV data was visualised using the plot and ring commands of the dphenome module.

In vitro growth experiments. Briefly, for individual growth curves, 10 ml of either LB-Lennox or defined minimal media was inoculated with 20 µl of a culture grown overnight in LB-Lennox broth. Cultures were grown at 37°C with shaking at 200 RPM and samples were removed at regular intervals to measure bioluminescence, using a VICTOR X Light Plate reader (Perkin Elmer), and viable counts, by plating onto LB-Lennox Agar (Fort Richard Laboratories Ltd., Auckland, New Zealand). Overnight cultures were plated to retrospectively to determine the initial inocula. Experiments were performed on seven separate occasions and results used to calculate Area Under Curve values for each strain. For the competition experiments, 10 µl of a culture grown overnight in LB-Lennox broth was used to inoculate 1 ml of defined minimal media, with the mixed culture tubes receiving 5 µl of each strain. Inoculated tubes were incubated overnight at 37°C with shaking at 200 RPM, followed by serial dilution in sterile phosphate buffered saline (PBS) for plating onto LB Agar containing either nalidixic acid or kanamycin. The ratio of colonies that grew on each antibiotic plate was used to determine the proportion of each strain remaining. Experiments were performed on eight separate occasions

and the results used to calculate Area Under Curve (AUC) values and competitive indices (CI). CI's were calculated as follows: CI = [strain of interest output/competing strain output]/[strain of interest input/competing strain input][30,31].

Infection of *Galleria mellonella*. 5th instar *Galleria mellonella* larvae (waxworms) were obtained from a commercial supplier (Biosuppliers.com, Auckland, New Zealand). Bacteria were grown overnight in LB-Lennox broth and used to infect waxworms which were pale in colour and weighed approximately 100-200 mg. Waxworms were injected into one of the last set of prolegs with 20 µl of approximately 10^8 CFU of bacteria using a 1ml fine needle insulin syringe. Waxworms were injected with either ICC169, ICC180 or a 1:1 mix and incubated at 37°C. Throughout the course of a 24 h infection, individual waxworms were inspected for phenotypic changes and scored using a standardised method for assessing waxworm health (the Caterpillar Health Index [CHI]) which we have developed. Briefly, waxworms were monitored for movement, cocoon formation, melanisation, and survival. Together, these data form a numerical scale, with lower CHI scores corresponding with more serious infections and higher scores with healthier waxworms. Scores were used to calculate AUC values. Bioluminescence (given as relative light units [RLU]) was measured at regular intervals from waxworms infected with ICC180. Waxworms were placed into individual wells of a dark OptiPlate-96 well microtitre plate (Perkin Elmer) and bioluminescence measured for 1 second to provide relative light units (RLU)/second using the VICTOR X Light Plate reader. Waxworms infected with ICC169 were used as a control. Following death, or at 24 h, waxworms were homogenised in PBS and plated onto LB-Lennox Agar containing the appropriate antibiotics. Independent experiments were performed three times using 10 waxworms per group.

Infection of Mice. Female 6-7 week old C57BL/6Elite mice were provided by the Vernon Jansen Unit (University of Auckland) from specific-pathogen free (SPF) stocks. All animals were

housed in individually HEPA-filtered cages with sterile bedding and free access to sterilised food water. Experiments were performed in accordance with the New Zealand Animal Welfare Act (1999) and institutional guidelines provided by the University of Auckland Animal Ethics Committee, which reviewed and approved these experiments under applications R1003 and R1496. Bacteria grown overnight in LB-Lennox broth were spun at 4500 RPM for 5 minutes, and resuspended in a tenth of the volume of sterile PBS, producing a 10x concentrated inoculum. Animals were orally inoculated using a gavage needles with 200 µl of either ICC169, ICC180, or a 1:1 mix (containing approximately 10^8 CFU of bacteria) and biophotonic imaging used to determine correct delivery of bacteria to the stomach. The number of viable bacteria used as an inoculum was determined by retrospective plating onto LB-Lennox Agar containing either nalidixic acid or kanamycin. Stool samples were recovered aseptically at various time points after inoculation, and the number of viable bacteria per gram of stool was determined after homogenisation at 0.1 g ml^{-1} in PBS and plating onto LB-Lennox Agar containing the appropriate antibiotics. The number and ratio of colonies growing on each antibiotic was used to calculate AUC values and CI's as described above. Independent experiments were performed twice using 6 animals per group.

In vivo bioluminescence imaging. Biophotonic imaging was used to noninvasively measure the bioluminescent signal emitted by *C. rodentium* ICC180 from anaesthetised mice to provide information regarding the localisation of the bacterium. Prior to being imaged, the abdominal area of each mouse was shaved, using a Vidal Sasoon handheld facial hair trimmer, to minimise any potential signal impedance by melanin within pigmented skin and fur. Bioluminescence (given as photons $second^{-1}$ cm^{-2} steradian $[sr]^{-1}$) was measured after gaseous anaesthesia with isoflurane using the IVIS® Kinetic camera system (Perkin Elmer). A photograph (reference image) was taken under low illumination before quantification of photons emitted from ICC180 at a binning of four over 1 minute using the Living Image software (Perkin

Elmer). The sample shelf was set to position D (field of view, 12.5 cm). For anatomic localisation, a pseudocolor image representing light intensity (blue, least intense to red, most intense) was generated using the Living Image software and superimposed over the gray-scale reference image. Bioluminescence in specific regions of individual mice also was quantified using the region of interest tool in the Living Image software program (given as photons second^{-1}) and used to calculate AUC values for each individual animal.

Statistical analyses. Data was analysed using GraphPad Prism 6. Data was tested for normality using the D'Agostino-Pearson test; data which failed normality was analysed using a non-parametric test, while data which passed normality was analysed using a parametric test. One-tailed tests were used to test the hypothesis that constitutively expressing light gives ICC180 a differential fitness cost compared to the non-bioluminescent parent strain ICC169. When comparing multiple experimental groups, Dunn's post hoc multiple comparison test was applied.

Results

Bioluminescent *Citrobacter rodentium* strain ICC180 has three altered chromosomal genes and a large deletion in plasmid pCROD1 in addition to insertion of the *lux* operon and kanamycin resistance gene.

We determined the whole genome draft sequences of *C. rodentium* ICC169 and ICC180 using Illumina sequence data. Compared with sequenced type strain ICC168 (Genbank accession number FN543502.1), both strains have a substitution of a guanine (G) to an adenine (A) residue at 2,475,894 bp, resulting in an amino acid change from serine (Ser) to phenylalanine (Phe) within *gyrA*, the DNA gyrase subunit, and conferring resistance to nalidixic acid. The sequencing data indicate that the *lux* operon and kanamycin resistance gene (a 7,759 bp fragment) has inserted at 5,212,273 bp, disrupting the coding region of a putative site-specific DNA recombinase (Figure 1). In addition to the presence of the *lux* operon and kanamycin resistance gene, we found that the genome of ICC180 differs from ICC169 by two single nucleotide polymorphisms (SNPs), a single base pair insertion (of a G residue at 3,326,092 bp which results in a frameshift mutation within *ROD*_31611, a putative membrane transporter) and a 90 bp deletion in *deoR* (deoxyribose operon repressor) (Table 1). All four plasmids previously described for *C. rodentium* were present in ICC180, however the largest of these plasmids, pCROD1, shows evidence of extensive deletion events and is missing 41 out of 60 genes (Supplementary Table 2).

Constitutive light expression does not have a great impact on the metabolism of *C. rodentium* ICC180.

C. rodentium ICC169 and its bioluminescent derivative ICC180 were grown on two separate occasions using PM plates 1-20. We analysed the data using the DuctApe software suite which calculates an activity index (AV) for each strain in response to each well. The AV values for

ICC169 and ICC80 are given as colour stripes going from red (AV = 0 [not active]) to green (AV = 6 [active]; 7 total k-means clusters) (Fig. 2).

Next, the growth curve data were transformed into Signal Values (SVs) as previously described[26], summarising the growth of each strain over time for each well. Wells which were considered to be actively respiring were analysed using the moderated t-test implemented in the limma R/Bioconductor package[28]. Those wells with a Benjamini-Hochberg corrected P-value of less than 0.05 are shown in Table 2 (with corresponding growth curves in Supplementary Fig. 2). Our results indicate that the growth of the two strains significantly differed ($p = <0.05$) in 26/1,920 wells. Of these >80% are from the PM11-20 plates, which belong to the chemical category, suggesting that the expression of bioluminescence is near-neutral in almost every non-toxic environment. The bioluminescent strain ICC180 is able to use D-glucosamine, cytidine and Ala-His as nitrogen sources, and inositol hexaphosphate as a phosphate source, and grew significantly better than ICC169 in the presence of 11 chemicals: the antibiotics kanamycin, paromomycin, geneticin, spiramycin, rolitetracycline, doxycycline, cefoxitin; the quaternary ammonium salt dequalinium chloride; coumarin; iodonitrotetrazolium violet; and the acetaldehyde dehydrogenase inhibitor disulphiram (Table 2). That the expression of a kanamycin resistance gene also improves growth of ICC180 in the presence of related aminoglycosides is reassuring. In contrast, the wildtype strain ICC169 was able to use the nitrogen peptide Lys-Asp and grew significantly better in the presence of 8 chemicals: the metal chelators, EDTA and EGTA, sodium nitrate, the antibiotics rifampicin and phenethicillin, the fungicide oxycarboxin, the cyclic polypeptide colistin, the nucleoside analogue cytosine-1-b-D-arabinofuranoside and (Table 2). The fact that significant differences in growth rate were observed for so few conditions, provided robust and comprehensive evidence that light production is near-neutral in *C. rodentium* ICC180.

The growth of ICC180 is not impaired during growth in rich laboratory media, when compared to its non-bioluminescent parent strain, but does exhibit an increased lag phase when grown in restricted media.

We grew ICC180 and ICC169 in rich (LB-Lennox) and restricted (minimal A salts with 1% glucose supplementation) laboratory media. For ICC180, we found that bioluminescence strongly correlated with the bacterial counts recovered throughout the growth period in both rich media (Spearman's r = 0.9293 [95% CI = 0.8828 - 0.9578], p = <0.0001) and minimal media (Spearman's r = 0.9440 [95% CI = 0.9001 - 0.9689], p = <0.0001) (Fig. 3A & B, 4A & B). We also found that the growth of each strain was comparable in rich media, with no significant difference between the bacterial counts recovered over 8 hours (Fig. 3B), as demonstrated by the calculated AUC values (Fig. 3C).

In contrast, we found a significant difference between the AUC values calculated from the bacterial counts recovered from ICC180 and ICC169 growing in restricted media (p = 0.0078, one-tailed Wilcoxon matched-pairs signed rank test) (Fig. 4C), suggesting that the bioluminescent strain would be at a competitive disadvantage in this medium. We calculated the slopes of the growth curves and found that there was no difference in the rates of growth of the two strains during exponential phase. Instead, we found a significant difference between the slopes calculated during the first 4 hours of growth (1/slope values: ICC169 = 1.48×10^{-7} [SD 9.98×10^{-8}], ICC180 = 2.47×10^{-7} [SD 1.10×10^{-7}]; p = 0.0041, one-tailed Paired *t* test), suggesting ICC180 spends longer in lag phase than ICC169 when grown in restricted media.

ICC180 is not impaired in the *Galleria mellonella* infection model.

We infected larvae of the Greater Wax Moth *G. mellonella* (waxworms) with ICC169 and ICC180 in single and 1:1 mixed infections. We monitored the waxworms over a 24-48 hour period for survival and disease symptoms. The Caterpillar Health Index (CHI) is a numerical

scoring system which measures degree of melanisation, silk production, motility, and mortality. We found that the majority of infected waxworms succumb to *C. rodentium* infection (Fig. 5A), which is reflected by the concurrent decrease in CHI score (Fig. 5B). This is in contrast to waxworms injected with PBS, who all survived and consistently scored 9-10 on the CHI scale throughout the experiments. We also found that the survival and symptoms of waxworms infected with each strain were comparable, with no significant difference between the survival curves (Fig. 5A), and calculated AUC values for the CHI scores (Fig. 5C). However, when we directly compared ICC169 and ICC180 in mixed infections of approximately 1:1, we found a significant difference in the relative abundance of the bacteria recovered from waxworms at either time of death or 24 hours, whichever occurred first ($p = 0.001$, one-tailed Wilcoxon matched-pairs signed rank test). Despite a slightly lower infectious dose, higher numbers of ICC180 were consistently recovered from infected waxworms (Fig. 5D).

ICC180 is impaired in mixed but not in single infections in mice when compared to its non-bioluminescent parent strain.

We orally gavaged groups of female 6-8 week old C57Bl/6 mice (n=6) with ~5 x 10^9 CFU of ICC169 and ICC180, either individually or with a 1:1 ratio of each strain. We followed the infection dynamics by obtaining bacterial counts from stool samples (Fig. 6) and by monitoring bioluminescence from ICC180 using biophotonic imaging (Fig. 7). We found that the growth of each strain was comparable during single infections, with no significant difference between the bacterial counts recovered throughout the infection (Fig. 6A), as demonstrated by the calculated AUC values (Fig. 6B).

In contrast, we found a significant difference between the Area Under Curve values calculated from the bacterial counts recovered from ICC180 and ICC169 during mixed infections ($p = 0.001$, one-tailed Wilcoxon matched-pairs signed rank test) (Fig. 6D). Our data demonstrates

that when in direct competition with ICC169, ICC180 is shed at consistently lower numbers from infected animals (Fig. 6C). At the peak of infection (days 6-8), this equates to over a 10-fold difference, with mice shedding a median of 1.195×10^8 CFU (SD 4.544×10^7) for ICC169 compared to 9.98×10^6 CFU (SD 1.544×10^7) for ICC180. This disadvantage is reflected in the Competitive Indices we calculated from bacterial counts recovered at each time point, which for ICC180 decreases steadily throughout the course of the infection (Fig. 6E). Despite this disadvantage, ICC180 is never completely outcompeted and remains detectable in the stools of infected animals until the clearance of infection (Fig. 6C), and by biophotonic imaging until day 10-13 post-infection (Fig. 7A).

Discussion

Bioluminescently-labelled bacteria have gained popularity as a powerful tool for investigating microbial pathogenicity in vivo, and for preclinical drug and vaccine development[32–35]. Individual infected and/or treated animals can be followed over time, in contrast to the large numbers of animals that are euthanised at specific time points of interest for quantifying bacterial loads using labour-intensive plate count methods. Most widely used is the *lux* operon of the terrestrial bacterium *P. luminescens*, which encodes for the luciferase enzyme which catalyses the bioluminescence reaction, and for a multi-enzyme complex responsible for regenerating the required substrate. As $FMNH_2$ is also required for light production, it is generally hypothesised that light production is likely to impose a metabolic burden on tagged bacteria.

The impact of expression of the *lux* operon has been reported for a number of microbial species. Sanz and colleagues created strains of *Bacillus anthracis* that emit light during germination, by introducing plasmids with *lux* operon expression driven by the *sspB* promoter [36]. The authors noted that the bioluminescent strains were less efficient at germinating, resulting in

371 an increase in the dose required to cause a lethal infection in mice inoculated by either the
372 subcutaneous or intranasal route. Despite the reduced virulence, bioluminescent *B. anthracis*
373 was still capable of successfully mounting an infection, and the use of biophotonic imaging
374 revealed new infection niches which would have been difficult to accurately measure using
375 traditional plating methods. Similarly, a clinical M75 isolate of *Streptococcus pyogenes* with the
376 *lux* operon chromosomally inserted at the *spy0535* gene was found to have significantly
377 attenuated maximal growth in vitro, as well as reduced survival in an intranasal mouse model [37].
378 The bioluminescent *Listeria monocytogenes* Xen32 strain was shown to have reduced mortality
379 after oral inoculation of BALB/cJ mice, however subsequent investigation revealed that the
380 chromosomally-located *lux* operon had inserted into the *flaA* gene, disrupting the ability of
381 Xen32 to produce flagella. This suggests that the virulence attenuation observed is likely due to
382 the location of the *lux* operon rather than the metabolic cost of light production[38].

383

384 In this study, we have compared a bioluminescent-derivative of the mouse enteropathogen *C.*
385 *rodentium*, strain ICC180, with its non-bioluminescent parent strain ICC169, using the BIOLOG
386 Phenotypic Microarray (PM) system, which tests microbial growth under approximately 2000
387 different metabolic conditions. Rather surprisingly, our results demonstrated that the expression
388 of bioluminescence in ICC180 is near-neutral in almost every non-toxic environment tested,
389 suggesting that light production is not metabolically costly to *C. rodentium*. This supports the
390 “free lunch hypothesis” proposed by Falls and colleagues, namely that cells have an excess of
391 metabolic power available to them [39]. Interestingly, ICC180 grew significantly better than its non-
392 bioluminescent parent strain in the presence of a number of different chemicals, including
393 several antibiotics, supporting previous findings that bacteria have many pleiotropic ways to
394 resist toxins[40]. In the case of the artificial electron acceptor iodonitrotetrazolium violet, we

hypothesise that light production may be altering the redox balance of the cell, thus making the dye less toxic.

We also compared the ability of ICC180 and ICC169 to directly compete with one another during infection of their natural host, laboratory mice, as well as larvae of the Greater Wax Moth *G. mellonella* (waxworms). Wax worms are becoming an increasingly popular surrogate host for infectious diseases studies due to legislative requirements in many countries to replace the use of animals in scientific research. Wax worms have a well-developed innate immune system involving a cellular immune response in the form of haemocytes, and a humoral immune response in the form of antimicrobial peptides in the hemolymph[41]. Detection of bacterial cell wall components leads to activation of the prophenoloxidase cascade, which is similar to the complement system in mammals [42], and subsequent endocytosis of bacteria by haemocytes. The haemocytes function in a similar way to mammalian neutrophils, and kill bacteria via NADPH oxidase and production of reactive oxygen species [43]. Again, we observed no fitness costs to constitutive light production by ICC180. Interestingly, we recovered significantly more ICC180 from wax worms infected with both ICC180 and ICC169. Similar to the response to iodonitrotetrazolium violet, an altered redox balance caused by light production could make reactive oxygen species generated by the wax worm immune response, less toxic.

In contrast, our data shows that the non-bioluminescent parent strain ICC169 has a clear competitive advantage over ICC180 during infection of adult C57Bl/6 mice, with the bioluminescent strain shed from infected animals at consistently lower numbers. Surprisingly though, this competitive advantage is not sufficient for the parent strain to outcompete and displace its bioluminescent derivative, which remains present in the gastrointestinal tract until clearance of both strains by the immune system. This suggests that there are sufficient niches

420 within the gastrointestinal tract for the two strains to coexist. This also leads us to conclude that,
421 while ICC180 does have a fitness disadvantage, it is negligible.

422

423 It is important to note that in addition to light production, ICC180 differs from its non-
424 bioluminescent parent strain ICC169 by lacking a putative site-specific DNA recombinase,
425 disrupted by insertion of the *lux* operon. *C. rodentium* ICC180 was constructed by random
426 transposon mutagenesis of ICC169 with a mini-Tn5 vector containing an unpromoted *lux* operon
427 and kanamycin-resistance gene. As an aside, previous characterisation of the site of insertion of
428 the *lux* operon suggested that the transposon had inserted within a homologue of the *xylE* gene.
429 However, whole genome sequencing has revealed that this was incorrect and the *lux* operon
430 has inserted at 5,212,273 bp, disrupting the coding region of the putative site-specific DNA
431 recombinase. Whole genome sequencing also revealed that ICC180 differs from ICC169 by 2
432 non-synonymous SNPs, a single base pair insertion and a 90 bp deletion. It is unclear if these
433 changes occurred during the process of transposon mutagenesis, and are merely 'hitch-hikers',
434 or after laboratory passage. The single base pair insertion revealed by sequencing is of a G
435 residue at 3,326,092 bp which results in a frameshift mutation within a putative membrane
436 transporter, while the 90 bp deletion is within the deoxyribose operon repressor gene *deoR*. The
437 DeoR protein represses the *deoCABD* operon, which is involved in the catabolism of
438 deoxyribonucleotides. One SNP is the substitution of an aspartic acid (D) for a glycine (G) at
439 residue 471 of Cts1V, a Type 6 secretion system protein involved in ATP binding. The other
440 SNP is the substitution of a glutamic acid (E) for a glycine (G) at residue 89 of the formate
441 acetyletransferase 2 gene *pflD,* which is involved in carbon utilisation under anaerobic
442 conditions. Modelling suggests that once mutated, residue 89 will be unable to make several
443 key contacts, suggesting the function of PflD will be affected. As we have not introduced these
444 genetic differences into the non-bioluminescent parent strain, we cannot be certain that the

fitness costs we observed are not a result of any single or combination of these differences, rather than expression of the *lux* operon. In addition, at 54 kb the largest *C. rodentium* plasmid pCROD1 is dramatically altered in ICC180, missing 41 out of 60 of genes. This is in contrast to previous results which indicated that pCROD1 is entirely absent in ICC180 [44]. We do not anticipate that the loss of a large part of this plasmid will have any significant impact however, as it has been shown that pCROD1 is frequently lost in *C. rodentium*, and that strains lacking pCROD1 do not show any attenuation of virulence in a C57BL/6 mouse model [44].

In conclusion, our data suggests that constitutive light expression is surprisingly neutral in *C. rodentium*, and while it may confer a fitness disadvantage, it is negligible. This supports the view that bioluminescent versions of microbes can be used as a substitute for their non-bioluminescent parents, at least in theory. In reality, the actual fitness costs will likely depend on the host bacterial species, whether the *lux* operon is located on a multi-copy plasmid or integrated into the chromosome (and if chromosomal, the site of insertion of the operon), and the levels of expression of the *lux* genes.

References

1. Vencl, F. V. Allometry and proximate mechanisms of sexual selection in photinus fireflies, and some other beetles. Integr. Comp. Biol. 44, 242–9 (2004).
2. Meyer-Rochow, V. B. Glowworms: a review of Arachnocampa spp. and kin. Luminescence 22, 251–65 (2007).
3. Jones, B. W. & Nishiguchi, M. K. Counterillumination in the Hawaiian bobtail squid, *Euprymna scolopes* Berry (Mollusca: Cephalopoda). Mar. Biol. 144, 1151–1155 (2004).

469 4. De Wet, J. R., Wood, K. V., Helinski, D. R. & DeLuca, M. Cloning of firefly luciferase cDNA
470 and the expression of active luciferase in *Escherichia coli*. Proc. Natl. Acad. Sci. U.S.A.
471 82, 7870–3 (1985).
472 5. Engebrecht, J., Nealson, K. & Silverman, M. Bacterial bioluminescence: isolation and
473 genetic analysis of functions from *Vibrio fischeri*. Cell 32, 773–81 (1983).
474 6. Szittner, R. & Meighen, E. Nucleotide sequence, expression, and properties of luciferase
475 coded by *lux* genes from a terrestrial bacterium. J. Biol. Chem. 265, 16581–7 (1990).
476 7. Andreu, N., Zelmer, A. & Wiles, S. Noninvasive biophotonic imaging for studies of
477 infectious disease. FEMS Microbiol. Rev. 35, 360–94 (2011).
478 8. Andreu, N., Zelmer, A., Sampson, S. L., Ikeh, M., Bancroft, G. J., Schaible, U. E., Wiles,
479 S. & Robertson B. D. Rapid in vivo assessment of drug efficacy against *Mycobacterium*
480 *tuberculosis* using an improved firefly luciferase. J. Antimicrob. Chemother. 68, 2118–27
481 (2013).
482 9. Andreu, N., Fletcher, T., Krishnan, N., Wiles, S. & Robertson, B. D. Rapid measurement of
483 antituberculosis drug activity in vitro and in macrophages using bioluminescence. J.
484 Antimicrob. Chemother. 67, 404–14 (2012).
485 10. Hastings & Presswood. Bacterial luciferase: $FMNH_2$-aldehyde oxidase. Meth. Enzymol.
486 53, 558–70 (1978).
487 11. Wiles, S., Clare, S., Harker, J., Huett, A., Young, D., Dougan, G. & Frankel, G. Organ
488 specificity, colonization and clearance dynamics in vivo following oral challenges with the
489 murine pathogen *Citrobacter rodentium*. Cell. Microbiol. 6, 963–72 (2004). Erratum: Cell.
490 Microbiol. 7, 459 (2005).
491 12. Mundy, R., MacDonald, T. T., Dougan, G., Frankel, G. & Wiles, S. *Citrobacter rodentium*
492 of mice and man. Cell. Microbiol. 7, 1697–706 (2005).

493 13. Collins, J. W., Keeney, K. M., Crepin, V. F., Rathinam, V. A., Fitzgerald, K. A., Finlay, B.
494 B. & Frankel, G. *Citrobacter rodentium*: infection, inflammation and the microbiota. Nat.
495 Rev. Microbiol. 12, 612–23 (2014).
496 14. Wiles, S., Pickard, K. M., Peng, K., MacDonald, T. T. & Frankel, G. In vivo
497 bioluminescence imaging of the murine pathogen *Citrobacter rodentium*. Infect. Immun.
498 74, 5391–6 (2006).
499 15. Wiles, S., Dougan, G. & Frankel, G. Emergence of a 'hyperinfectious' bacterial state after
500 passage of *Citrobacter rodentium* through the host gastrointestinal tract. Cell. Microbiol. 7,
501 1163–72 (2005).
502 16. Winson, M. K., Swif.t S., Hill, P. J., Sims, C. M., Griesmayr, G., Bycroft, B. W., Williams, P.
503 & Stewart, G.S. Engineering the *luxCDABE* genes from *Photorhabdus luminescens* to
504 provide a bioluminescent reporter for constitutive and promoter probe plasmids and mini-
505 Tn*5* constructs. FEMS Microbiol. Lett. 163, 193–202 (1998).
506 17. Bochner, B. R., Gadzinski, P. & Panomitros, E. Phenotype microarrays for high-
507 throughput phenotypic testing and assay of gene function. Genome Res. 11, 1246–55
508 (2001).
509 18. Davis, B. D. The isolation of biochemically deficient mutants of bacteria by means of
510 penicillin. Proc. Natl. Acad. Sci. U.S.A. 35, 1–10 (1949).
511 19. Cox, M. P., Peterson, D. A. & Biggs, P. J. SolexaQA: At-a-glance quality assessment of
512 Illumina second-generation sequencing data. BMC Bioinformatics 11, 485 (2010).
513 20. Petty, N. K., Bulgin, R., Crepin, V. F., Cerdeño-Tárraga, A. M., Schroeder, G. N., Quail, M.
514 A., Lennard, N., Corton, C., Barron, A., Clark, L., Toribio, A. L., Parkhill, J., Dougan, G.,
515 Frankel, G. & Thomson, N. R. The *Citrobacter rodentium* genome sequence reveals
516 convergent evolution with human pathogenic *Escherichia coli*. J. Bacteriol. 192, 525–38
517 (2010).

21. Li, H. & Durbin, R. Fast and accurate long-read alignment with Burrows-Wheeler transform. Bioinformatics 26, 589–95 (2010).
22. Li, H., Handsaker, B., Wysoker, A., Fennell, T., Ruan, J., Homer, N., Marth, G., Abecasis, G., Durbin, R.; 1000 Genome Project Data Processing Subgroup. The Sequence Alignment/Map format and SAMtools. Bioinformatics 25, 2078–9 (2009).
23. Deatherage, D. E. & Barrick, J. E. Identification of mutations in laboratory-evolved microbes from next-generation sequencing data using breseq. Methods Mol. Biol. 1151, 165–88 (2014).
24. Hernandez, D., François, P., Farinelli, L., Osterås, M. & Schrenzel, J. De novo bacterial genome sequencing: millions of very short reads assembled on a desktop computer. Genome Res. 18, 802–9 (2008).
25. Kearse, M., Moir, R., Wilson, A., Stones-Havas, S., Cheung, M., Sturrock, S., Buxton, S., Cooper, A., Markowitz, S., Duran, C., Thierer, T., Ashton, B., Meintjes, P. & Drummond, A. Geneious Basic: an integrated and extendable desktop software platform for the organization and analysis of sequence data. Bioinformatics 28, 1647–9 (2012).
26. Reuter, S., Connor, T. R., Barquist, L., Walker, D., Feltwell, T., Harris, S. R., Fookes, M., Hall, M. E., Petty, N. K., Fuchs, T. M., Corander, J., Dufour, M., Ringwood, T., Savin, C., Bouchier, C., Martin, L., Miettinen, M., Shubin, M., Riehm, J. M., Laukkanen-Ninios, R., Sihvonen, L. M., Siitonen, A., Skurnik, M., Falcão, J. P., Fukushima, H., Scholz, H. C., Prentice, M. B., Wren, B. W., Parkhill, J., Carniel, E., Achtman, M., McNally, A. & Thomson, N.R. Parallel independent evolution of pathogenicity within the genus *Yersinia*. Proc. Natl. Acad. Sci. U.S.A. 111, 6768–73 (2014).
27. Homann, O. R., Cai, H., Becker, J. M. & Lindquist, S. L. Harnessing natural diversity to probe metabolic pathways. PLOS Genet. 1, e80 (2005).
28. Smyth, G. K. Linear models and empirical bayes methods for assessing differential expression in microarray experiments. Stat. Appl. Genet. Mol. Biol. 3, Article3 (2004).

544 29. Galardini, M., Mengoni, A., Biondi, E. G., Semeraro, R., Florio, A., Bazzicalupo, M.,
545 Benedetti, A. & Mocali, S. DuctApe: A suite for the analysis and correlation of genomic
546 and OmniLogTM Phenotype Microarray data. Genomics 103, 1-10 (2014).
547 30. Freter, R., O'Brien, P. C. & Macsai, M. S. Role of chemotaxis in the association of motile
548 bacteria with intestinal mucosa: in vivo studies. Infect. Immun. 34, 234–40 (1981).
549 31. Taylor, R. K., Miller, V. L., Furlong, D. B. & Mekalanos, J. J. Use of *phoA* gene fusions to
550 identify a pilus colonization factor coordinately regulated with cholera toxin. Proc. Natl.
551 Acad. Sci. U.S.A. 84, 2833–7 (1987).
552 32. Sun, Y., Connor, M. G., Pennington, J. M. & Lawrenz, M. B. Development of
553 bioluminescent bioreporters for in vitro and in vivo tracking of *Yersinia pestis*. PLOS One
554 7, e47123 (2012).
555 33. Massey, S., Johnston, K., Mott, T. M., Judy, B. M., Kvitko, B. H., Schweizer, H. P., Estes,
556 D. M. & Torres, A. G. In vivo bioluminescence imaging of *Burkholderia mallei* respiratory
557 infection and treatment in the mouse model. Front. Microbiol 2, 174 (2011).
558 34. Steinhuber, A., Landmann, R., Goerke, C., Wolz, C. & Flückiger, U. Bioluminescence
559 imaging to study the promoter activity of *hla* of *Staphylococcus aureus* in vitro and in vivo.
560 Int. J. Med. Microbiol. 298, 599–605 (2008).
561 35. Kassem, I. I., Splitter, G. A., Miller, S. & Rajashekara, G. Let there be light!
562 Bioluminescent imaging to study bacterial pathogenesis in live animals and plants. Adv.
563 Biochem. Eng. Biotechnol. 154, 119–45 (2016).
564 36. Sanz, P., Teel, L. D., Alem, F., Carvalho, H. M., Darnell, S. C. & O'Brien, A. D. Detection
565 of *Bacillus anthracis* spore germination in vivo by bioluminescence imaging. Infect.
566 Immun. 76, 1036–47 (2008).
567 37. Alam, F. M., Bateman, C., Turner, C. E., Wiles, S. & Sriskandan, S. Non-invasive
568 monitoring of *Streptococcus pyogenes* vaccine efficacy using biophotonic imaging. PLOS
569 One 8, e82123 (2013).

38. Bergmann, S., Rohde, M., Schughart, K. & Lengeling, A. The bioluminescent *Listeria monocytogenes* strain Xen32 is defective in flagella expression and highly attenuated in orally infected BALB/cJ mice. Gut. Pathog. 5, 19 (2013).
39. Falls, K., Williams, A., Bryksin, A. & Matsumura, I. *Escherichia coli* deletion mutants illuminate trade-offs between growth rate and flux through a foreign anabolic pathway. PLOS One 9, e88159 (2014).
40. Soo, V. W., Hanson-Manful, P. & Patrick, W. M. Artificial gene amplification reveals an abundance of promiscuous resistance determinants in *Escherichia coli*. Proc. Natl. Acad. Sci. U.S.A. 108, 1484–9 (2011).
41. Vogel, H., Altincicek, B., Glöckner, G. & Vilcinskas, A. A comprehensive transcriptome and immune-gene repertoire of the lepidopteran model host *Galleria mellonella*. BMC Genomics 12, 308 (2011).
42. Park, S., Kim, C. H., Jeong, W. H., Lee, J. H., Seo, S. J., Han, Y. S. & Lee, I. H. Effects of two hemolymph proteins on humoral defense reactions in the wax moth, *Galleria mellonella*. Dev. Comp. Immunol. 29, 43–51 (2005).
43. Bergin, D., Reeves, E., Renwick, J., Wientjes, F. & Kavanagh, K. Superoxide production in *Galleria mellonella* hemocytes: identification of proteins homologous to the NADPH oxidase complex of human neutrophils. Infect. Immun. 73, 4161–4170 (2005).
44. Petty, N. K., Feltwell, T., Pickard, D., Clare, S., Toribio, A. L., Fookes, M., Roberts, K., Monson, R., Nair, S., Kingsley, R. A., Bulgin, R., Wiles, S., Goulding, D., Keane, T., Corton, C., Lennard, N., Harris, D., Willey, D., Rance, R., Yu, L., Choudhary, J. S., Churcher, C., Quail, M. A., Parkhill, J., Frankel, G., Dougan, G., Salmond, G. P. & Thomson, N. R. *Citrobacter rodentium* is an unstable pathogen showing evidence of significant genomic flux. PLOS Path. 7, e1002018 (2011).

Acknowledgements

This work was supported by seed funding from the Maurice Wilkins Centre for Molecular Biodiscovery, and by a Sir Charles Hercus Fellowship to SW (09/099) from the Health Research Council of New Zealand. LB is supported by a Research Fellowship from the Alexander von Humboldt Stiftung/Foundation.

Tables

Position	Base change	Amino acid change	Gene	Function
2,936,285	T→C	D471G (GAC→GGC)	*cts1V*	T6SS protein Cts1V
3,999,002	T→C	E89G (GAG→GGG)	*pflD*	Formate acetyltransferase 2
3,326,092	CAG→ CAGG	Frameshift	*ROD_ 31611*	Major Facilitator Superfamily transporter

Table 1. SNPs and indels that differ between the bioluminescent *C. rodentium* derivative ICC180 and its parent strain ICC169. Sequencing revealed three points of difference between ICC180 and ICC169. Two SNPs are present, each cytosine substitutions, and one guanine insertion inducing a frameshift mutation. Sequencing data was analysed using BreSeq[23].

615

616

PM Class	Substrate	Adjusted p value	Improved growth by ICC169	Improved growth by ICC180	Comment
Nitrogen	D-glucosamine	0.0159		✔	
	Cytidine	0.0280		✔	
	Ala-His	0.0316		✔	
Phosphate	Inositol hexaphosphate	0.0280		✔	
Nitrogen peptides	Lys-Asp	0.0306	✔		
Chemicals	Kanamycin	0.0076		✔	Conferred by KanR gene
	Paromomycin	0.0048		✔	Aminoglycoside -- the kanamycin cassette will be mediating resistance
	Geneticin	0.0048		✔	Aminoglycoside -- the kanamycin cassette will be mediating resistance
	Dequalinium chloride	0.0116		✔	Quaternary ammonium salt
	Spiramycin	0.0088		✔	Macrolide -- acts at ribosomal 50S, c.f. aminoglycosides at 30S
	Rolitetracycline	0.0316		✔	Tetracycline; prevents tRNA binding at 30S A-site
	Doxycycline	0.0210		✔	Tetracycline; prevents tRNA binding at 30S A-site
	Coumarin	0.0333		✔	Fragrant organic compound found in many plants
	Iodonitro tetrazolium violet (INT)	0.0087		✔	Electron acceptor, reduced by succinate dehydrogenase (and by superoxide radicals)
	EDTA	0.0048	✔		Metal chelator

	EGTA	0.0210	✔		Metal chelator
	Rifampicin	0.0048	✔		RNA polymerase inhibitor
	Colistin	0.0048	✔		Cyclic polypeptide; disrupts outer membrane
	Oxycarboxin	0.0121	✔		Fungicide
	Phenethicillin	0.0048	✔		Beta-lactam
	Cytosine-1-b-D-arabinofuranoside	0.0123	✔		Nucleoside analogue (anti-cancer/-viral)
	Sodium Nitrate	0.0306	✔		
	Cefoxitin	0.0316		✔	Beta-lactam
	Disulphiram	0.0349		✔	Inhibits acetaldehyde dehydrogenase

617

618 **Table 2. Phenotypic microarray (PM) wells in which the growth of bioluminescent *C.***
619 ***rodentium* derivative ICC180 significantly differs from its non-bioluminescent parent**
620 **strain ICC169.**

621

622 **Figure legends**

623

624 **Figure 1. Whole genome sequencing shows that the *lux* operon and kanamcyin**
625 **resistance gene have inserted at position 5,212,273 in the chromosome of *C. rodentium***
626 **ICC180, disrupting a putative site-specific DNA recombinase.**

627

628 **Figure 2. The growth of *C. rodentium* ICC180 compared to its non-bioluminescent parent**
629 **strain ICC169 as assessed by phenotypic microarray (PM).** Wildtype *C. rodentium* ICC169
630 and its bioluminescent derivative ICC180 were grown on two separate occasions using PM
631 plates 1-20. Activity rings from the PM data are shown where the grey inner circles indicate the
632 strains' order and the external circle indicates the PM categories (see Key). The activity index
633 (AV) was calculated for each strain in response to each well and the values for ICC169 are
634 shown as colour stripes going from red (AV = 0 [not active]) to green (AV = 6 [active]; 7 total k-
635 means clusters.

636

637 **Figure 3. *C. rodentium* ICC180 is not impaired during growth in rich laboratory media**
638 **when compared to its non-bioluminescent parent strain ICC169.** Wildtype *C. rodentium*
639 ICC169 (shown as purple circles) and its bioluminescent derivative ICC180 (shown as blue
640 triangles) were grown in LB-Lennox broth and monitored for changes in bioluminescence (given
641 as relative light units [RLU] ml^{-1}) (A) and bacterial counts (given as colony forming units [CFU]
642 ml^{-1}) (B). Bacterial count data was used to calculate Area Under Curve values for each strain
643 (C). Data (medians with ranges where appropriate) is presented from experiments performed on
644 eight separate occasions.

645

Figure 4. *C. rodentium* ICC180 is mildly impaired during growth in a defined minimal laboratory media when compared to its non-bioluminescent parent strain ICC169. Wildtype *C. rodentium* ICC169 (shown as purple circles) and its bioluminescent derivative ICC180 (shown as blue triangles) were grown in minimal A salts supplemented with 1% glucose and monitored for changes in bioluminescence (given as relative light units [RLU] ml^{-1}) (A) and bacterial counts (given as colony forming units [CFU] ml^{-1}) (B). Bacterial count data was used to calculate Area Under Curve values for each strain, which were found to be significantly different ($p=0.0078$; Wilcoxon Matched pairs-signed rank test) (C). Data (medians with ranges where appropriate) is presented from experiments performed on eight separate occasions.

Figure 5. Bioluminescent *C. rodentium* ICC180 is not impaired in the *Galleria mellonella* infection model. Groups of larvae (n = 10) of the Greater Wax Moth *Galleria mellonella* were infected with ICC169 and ICC180 in single and 1:1 mixed infections and monitored for survival (%) (A) and for disease symptoms using the Caterpillar Health Index (CHI), a numerical scoring system which measures degree of melanisation, silk production, motility, and mortality (given as median CHI values) (B). Survival curves (A) and calculated Area Under Curve data of CHI scores reveals no difference between waxworm response to infection from either strain (C). Waxworms infected with a 1:1 mix of ICC169 and ICC180 were homogenised at 24-hours, or at time of death if earlier. Actual infecting doses for each strain were determined by retrospective plating, and are indicated by *.The bacterial burden of ICC180 and ICC169 in individual caterpillars (indicated by the dotted line), was calculated after plating onto differential media and found to be significantly different ($p=0.001$; one-tailed Wilcoxon matched pairs-signed rank test) (D). Data (medians with ranges where appropriate) is presented from experiments performed on 3 separate occasions, except (A) and (D), where the results of a representative experiment are shown.

Figure 6. *C. rodentium* ICC180 is impaired during mixed, but not in single, infections in mice when compared to its non-bioluminescent parent strain ICC169. Groups of female 6-8 week old C57Bl/6 mice (n=6) were orally-gavaged with ~5 x 10^9 CFU of wildtype *C. rodentium* ICC169 (shown as purple circles) and its bioluminescent derivative ICC180 (shown as blue triangles) in single infections (A, B) or 1:1 mixed infections (C, D) and monitored for changes in bacterial counts (given as colony forming units [CFU] g^{-1} stool) (A, B). Bacterial count data was used to calculate Area Under Curve values for each strain in single (B) and mixed (D) infections, and were found to be significantly different only for the mixed infections ($p=0.001$; one-tailed Wilcoxon Matched pairs-signed rank test). This is reflected in the competitive indices (CI) calculated from the bacterial counts recovered during mixed infections, with ICC180 showing a growing competitive disadvantage from day 2 post-infection (E). Data (medians with ranges where appropriate) is presented from experiments performed on two separate occasions.

Figure 7. Despite having a fitness disadvantage in mixed infections of mice, ICC180 is still visible by biophotonic imaging. Groups of female 6-8 week old C57Bl/6 mice (n=6) were orally-gavaged with ~5 x 10^9 CFU of wildtype *C. rodentium* ICC169 and its bioluminescent derivative ICC180 in single infections or 1:1 mixed infections. Bioluminescence (given as photons $second^{-1}$ cm^{-2} sr^{-1}) from ICC180 was measured after gaseous anesthesia with isoflurane using the IVIS® Kinetic camera system (Perkin Elmer). A photograph (reference image) was taken under low illumination before quantification of photons emitted from ICC180 at a binning of four over 1 minute using the Living Image software (Perkin Elmer). The sample shelf was set to position D (field of view, 12.5 cm). The images show peak bioluminescence with variations in colour representing light intensity at a given location and superimposed over the grey-scale reference image (A). Red represents the most intense light emission, whereas blue corresponds to the weakest signal. The color bar indicates relative signal intensity (as photons/second/cm^2/steradian [Sr]). Bioluminescence from the abdominal region of individual

mice also was quantified using the region of interest tool in the Living Image software program (given as photons second^{-1}) and used to calculate Area Under Curve values for each individual animal (B). Dotted line represents background. Experiments were performed on two separate occasions. Three representative animals are shown.

Supplementary Fig. 1. Elbow tests of phenotypic microarray array data to determine the number of clusters appropriate for k-means clustering. Data was analysed using the DuctApe software suite.

Supplementary Fig. 2. The growth of *C. rodentium* ICC180 compared to its non-bioluminescent parent strain ICC169 as assessed by phenotypic microarray (PM). Wildtype *C. rodentium* ICC169 (shown as purple lines) and its bioluminescent derivative ICC180 (shown as blue lines) were grown on two separate occasions using PM plates 1-20 (categorised by colour [see Key]). Differences between the growth of ICC169 and ICC180 in each individual well were analysed using the moderated t-test provided by limma[28]. Wells in which the differences had an adjusted p-value of less than 0.5 (stringent cut-off) are shown.

Supplementary Fig. 3. Infection of larvae of the Greater Wax Moth *Galleria mellonella* with bioluminescent *C. rodentium* ICC180 can be visualised by luminometry. Groups of larvae (n = 10) of the Greater Wax Moth *Galleria mellonella* were infected with ~10^8 CFU of *C. rodentium* ICC169 or ICC180 and monitored for bioluminescence using a plate luminometer. Data (medians with ranges) is presented from experiments performed on 3 separate occasions and is given as relative light units [RLU] waxworm^{-1}.

722 **Supplementary Table 1. BIOLOG Phenotypic Microarray assays.**

PM1 – Carbon Sources	A1, Negative Control; A2, L-Arabinose; A3, N-Acetyl-D Glucosamine; A4, D-Saccharic Acid; A5, Succinic Acid; A6, D-Galactose; A7, L-Aspartic Acid; A8, L-Proline; A9, D-Alanine; A10, D-Trehalose; A11, D-Mannose; A12, Dulcitol; B1, D-Serine; B2, D-Sorbitol; B3, Glycerol; B4, L-Fucose; B5, D-Glucuronic Acid; B6, D-Gluconic Acid; B7, D,L-α-Glycerol Phosphate; B8, D-Xylose; B9, L-Lactic Acid; B10, Formic Acid; B11, D-Mannitol; B12, L-Glutamic Acid; C1, D-Glucose-6-Phosphate; C2, D-Galactonic Acid-γ-Lactone; C3, D,L-Malic Acid; C4, D-Ribose; C5, Tween 20; C6, L-Rhamnose; C7, D-Fructose; C8, Acetic Acid; C9, α-D-Glucose; C10, Maltose; C11, D-Melibiose; C12, Thymidine; D1, L-Asparagine; D2, D-Aspartic Acid; D3, D-Glucosaminic Acid; D4, 1,2- Propanediol; D5, Tween 40; D6, α -Keto-Glutaric Acid; D7, α -Keto-Butyric Acid; D8, α -Methyl-D Galactoside; D9, α -D-Lactose; D10, Lactulose; D11, Sucrose; D12, Uridine; E1, L-Glutamine; E2, m-Tartaric Acid; E3, D-Glucose-1-Phosphate; E4, D-Fructose-6-Phosphate; E5, Tween 80; E6, α-Hydroxy Glutaric Acid-α-Lactone; E7, α-Hydroxy Butyric Acid; E8, α-Methyl-DGlucoside; E9, Adonitol; E10, Maltotriose; E11, 2-Deoxy Adenosine; E12, Adenosine; F1, Glycyl-L-Aspartic Acid; F2, Citric Acid; F3, m-Inositol; F4, D-Threonine; F5, Fumaric Acid; F6, Bromo Succinic Acid; F7, Propionic Acid; F8, Mucic Acid; F9, Glycolic Acid; F10, Glyoxylic Acid; F11, D-Cellobiose; F12, Inosine; G1, Glycyl-L-Glutamic Acid; G2, Tricarballylic Acid; G3, L-Serine; G4, L-Threonine; G5,L-Alanine; G6, L-Alanyl-Glycine; G7, Acetoacetic Acid; G8, N-Acetyl-β-D-Mannosamine; G9, Mono Methyl Succinate; G10, Methyl Pyruvate; G11, D-Malic Acid; G12, L-Malic Acid; H1, Glycyl-L-Proline; H2, p-Hydroxy Phenyl Acetic Acid; H3, m-Hydroxy Phenyl Acetic Acid; H4, Tyramine; H5, D-Psicose; H6, L-Lyxose; H7, Glucuronamide; H8, Pyruvic Acid; H9, L-Galactonic Acid-γ-Lactone; H10, D-Galacturonic Acid; H11, Phenylethylamine; H12, 2-Amino Ethanol.
PM2 – Carbon Sources	A1, Negative Control; A2, Chondroitin Sulfate C; A3, α-Cyclodextrin; A4, β-Cyclodextrin; A5, γ-Cyclodextrin; A6, Dextrin; A7, Gelatin; A8, Glycogen; A9, Inulin; A10, Laminarin; A11, Mannan; A12, Pectin; B1, N-Acetyl-D Galactosamine; B2, N-Acetyl Neuraminic Acid; B3, β-D-Allose; B4, Amygdalin; B5, D-Arabinose; B6, D-Arabitol; B7, L-Arabitol; B8, Arbutin; B9, 2-Deoxy-D Ribose; B10, i-Erythritol; B11, D-Fucose; B12,3-0-β-D-Galactopyranosyl-D Arabinose; C1, Gentiobiose; C2, L-Glucose; C3, Lactitol; C4, D-Melezitose; C5, Maltitol; C6, a-Methyl-D Glucoside; C7, β-Methyl-D Galactoside; C8, 3-Methyl Glucose; C9, β -Methyl-D Glucuronic Acid; C10, α-Methyl-D Mannoside; C11, β -Methyl-D Xyloside; C12, Palatinose; D1, D-Raffinose; D2, Salicin; D3, Sedoheptulosan; D4, L-Sorbose; D5, Stachyose; D6, D-Tagatose; D7, Turanose; D8, Xylitol; D9, N-Acetyl-D Glucosaminitol; D10, γ-Amino Butyric Acid; D11, δ-Amino Valeric Acid; D12, Butyric Acid; E1, Capric Acid; E2, Caproic Acid; E3, Citraconic Acid; E4, Citramalic Acid; E5, D-Glucosamine; E6, 2-Hydroxy Benzoic Acid; E7, 4-Hydroxy Benzoic Acid; E8, β-Hydroxy Butyric Acid; E9, δ-Hydroxy Butyric Acid; E10, a-Keto-Valeric Acid; E11, Itaconic Acid; E12, 5-Keto-D Gluconic Acid; F1, D-Lactic Acid Methyl Ester; F2, Malonic Acid; F3, Melibionic Acid; F4, Oxalic Acid; F5, Oxalomalic Acid; F6, Quinic Acid; F7, D-Ribono-1,4-Lactone; F8, Sebacic Acid; F9, Sorbic Acid; F10, Succinamic Acid; F11, D-Tartaric Acid; F12, L-Tartaric Acid; G1, Acetamide; G2, L-Alaninamide; G3, N-Acetyl-L Glutamic Acid; G4, L-Arginine; G5, Glycine; G6, L-Histidine; G7, L-Homoserine; G8, Hydroxy-L Proline; G9, L-Isoleucine; G10, L-Leucine; G11, L-Lysine; G12, L-Methionine; H1, L-Ornithine; H2, L-Phenylalanine; H3, L-Pyroglutamic Acid; H4, L-Valine; H5, D,L-Carnitine; H6, Sec-Butylamine; H7, D.L-Octopamine; H8, Putrescine; H9, Dihydroxy Acetone; H10, 2,3-Butanediol; H11, 2,3-Butanone; H12, 3-Hydroxy 2-Butanone.
PM3 – Nitrogen Sources	A1, Negative Control; A2, Ammonia; A3, Nitrite; A4, Nitrate; A5, Urea; A6, Biuret; A7, L-Alanine; A8, L-Arginine; A9, L-Asparagine; A10, L-Aspartic Acid; A11, L-Cysteine; A12, L-

	Glutamic Acid; B1, L-Glutamine; B2, Glycine; B3, L-Histidine; B4, L-Isoleucine; B5, L-Leucine; B6, L-Lysine; B7, L-Methionine; B8, L-Phenylalanine; B9, L-Proline; B10, L-Serine; B11, L-Threonine; B12, L-Tryptophan; C1, L-Tyrosine; C2, L-Valine; C3, D-Alanine; C4, D-Asparagine; C5, D-Aspartic Acid; C6, D-Glutamic Acid; C7, D-Lysine; C8, D-Serine; C9, D-Valine; C10, L-Citrulline; C11, L-Homoserine; C12, L-Ornithine; D1, N-Acetyl-L Glutamic Acid; D2, N-Phthaloyl-L Glutamic Acid; D3, L-Pyroglutamic Acid; D4, Hydroxylamine; D5, Methylamine; D6, N-Amylamine; D7, N-Butylamine; D8, Ethylamine; D9, Ethanolamine; D10, Ethylenediamine; D11, Putrescine; D12, Agmatine; E1, Histamine; E2, β-Phenylethylamine; E3, Tyramine; E4, Acetamide; E5, Formamide; E6, Glucuronamide; E7, D,L-Lactamide; E8, D-Glucosamine; E9, D-Galactosamine; E10, D-Mannosamine; E11, N-Acetyl-D Glucosamine; E12, N-Acetyl-D Galactosamine; F1, N-Acetyl-D Mannosamine; F2, Adenine; F3, Adenosine; F4, Cytidine; F5, Cytosine; F6, Guanine; F7, Guanosine; F8, Thymine; F9, Thymidine; F10, Uracil; F11, Uridine; F12, Inosine; G1, Xanthine; G2, Xanthosine; G3, Uric Acid; G4, Alloxan; G5, Allantoin; G6, Parabanic Acid; G7, D,L-α-Amino-N Butyric Acid; G8, β-Amino-N Butyric Acid; G9, ε-Amino-N Caproic Acid; G10, D,L-α-Amino Caprylic Acid; G11, δ-Amino-N Valeric Acid; G12, α-Amino-N Valeric Acid; H1, Ala-Asp; H2, Ala-Gln; H3, Ala-Glu; H4, Ala-Gly; H5, Ala-His; H6, Ala-Leu; H7, Ala-Thr; H8, Gly-Asn; H9, Gly-Gln; H10, Gly-Glu; H11, Gly-Met; H12, Met-Ala.
PM4 – Phosphorus and Sulfur Sources	A1, Negative Control; A2, Phosphate; A3, Pyrophosphate; A4, Trimetaphosphate; A5, Tripolyphosphate; A6, Triethyl Phosphate; A7, Hypophosphite; A8, Adenosine-2'-monophosphate; A9, Adenosine-3'-monophosphate; A10, Adenosine-5'-monophosphate; A11, Adenosine-2',3'-cyclic monophosphate; A12, Adenosine-3',5'-cyclic monophosphate; B1, Thiophosphate; B2, Dithiophosphate; B3, D,L-α-Glycerol Phosphate; B4, β-Glycerol Phosphate; B5, Carbamyl Phosphate; B6, D-2-Phospho Glyceric Acid; B7, D-3-Phospho Glyceric Acid; B8, Guanosine-2'-monophosphate; B9, Guanosine-3'-monophosphate; B10, Guanosine-5'-monophosphate; B11, Guanosine-2',3'-cyclic monophosphate; B12, Guanosine-3',5'-cyclic monophosphate; C1, Phosphoenol Pyruvate; C2, Phospho Glycolic Acid; C3, D-Glucose-1-Phosphate; C4, D-Glucose-6-Phosphate; C5, 2-Deoxy-D Glucose 6-Phosphate; C6, D-Glucosamine-6-Phosphate; C7, 6-Phospho Gluconic Acid; C8, Cytidine-2'-monophosphate; C9, Cytidine-3'-monophosphate; C10, Cytidine-5'-monophosphate; C11, Cytidine-2',3'-cyclic monophosphate; C12, Cytidine-3',5'-cyclic monophosphate; D1, D-Mannose-1-Phosphate; D2, D-Mannose-6-Phosphate; D3, Cysteamine-S Phosphate; D4, Phospho-L Arginine; D5, O-Phospho-D Serine; D6, O-Phospho-L Serine; D7, O-Phospho-L Threonine; D8, Uridine-2'-monophosphate; D9, Uridine-3'-monophosphate; D10, Uridine-5'-monophosphate; D11, Uridine-2',3'-cyclic monophosphate; D12, Uridine-3',5'-cyclic monophosphate; E1, O-Phospho-D Tyrosine; E2, O-Phospho-L Tyrosine; E3, Phosphocreatine; E4, Phosphoryl Choline; E5, O-Phosphoryl Ethanolamine; E6, Phosphono Acetic Acid; E7, 2-Aminoethyl Phosphonic Acid; E8, Methylene Diphosphonic Acid; E9, Thymidine-3'-monophosphate; E10, Thymidine-5'-monophosphate; E11, Inositol Hexaphosphate; E12, Thymidine 3',5'-cyclic monophosphate; F1, Negative Control; F2, Sulfate; F3, Thiosulfate; F4, Tetrathionate; F5, Thiophosphate; F6, Dithiophosphate; F7, L-Cysteine; F8, D-Cysteine; F9, L-Cysteinyl Glycine; F10, L-Cysteic Acid; F11, Cysteamine; F12, L-Cysteine Sulfinic Acid; G1, N-Acetyl-L Cysteine; G2, S-Methyl-L Cysteine; G3, Cystathionine; G4, Lanthionine; G5, Glutathione; G6, D,L-Ethionine; G7, L-Methionine; G8, D-Methionine; G9, Glycyl-L Methionine; G10, N-Acetyl-D,L Methionine; G11, L- Methionine Sulfoxide; G12, L-Methionine Sulfone; H1, L-Djenkolic Acid; H2, Thiourea; H3, 1-Thio-β-D Glucose; H4, D,L-Lipoamide; H5, Taurocholic Acid; H6, Taurine; H7, Hypotaurine; H8, p-Amino Benzene Sulfonic Acid; H9, Butane Sulfonic Acid; H10, 2-Hydroxyethane Sulfonic Acid; H11, Methane Sulfonic Acid;

	H12, Tetramethylene Sulfone.
PM5 – Nutrient Supplements	A1, Negative Control; A2, Positive Control; A3, L-Alanine; A4, L-Arginine; A5, L-Asparagine; A6, L-Aspartic Acid; A7, L-Cysteine, A8, L-Glutamic Acid; A9, Adenosine-3',5'-cyclic monophosphate; A10, Adenine; A11, Adenosine; A12, 2'-Deoxy Adenosine; B1, L-Glutamine; B2, Glycine; B3, L-Histidine; B4, L-Isoleucine; B5, L-Leucine; B6, L-Lysine; B7, L-Methionine; B8, L-Phenylalanine; B9, Guanosine-3',5'-cyclic monophosphate; B10, Guanine; B11, Guanosine; B12, 2'-Deoxy Guanosine; C1, L-Proline; C2, L-Serine; C3, L-Threonine; C4, L-Tryptophan; C5, L-Tyrosine; C6, L-Valine; C7, L-isoleucine + L-Valine; C8, trans-4-Hydroxy L-Proline; C9, (5) 4-AminoImidazole-4(5)-Carboxamide; C10, Hypoxanthine; C11, Inosine; C12, 2'-Deoxy Inosine; D1, L-Ornithine; D2, L-Citrulline; D3, Chorismic Acid; D4, (-)Shikimic Acid; D5, L-Homoserine Lactone; D6, D-Alanine; D7, D-Aspartic Acid; D8, D-Glutamic Acid; D9, D,L-α,ε-Diaminopimelic Acid; D10, Cytosine; D11, Cytidine; D12, 2'-Deoxy Cytidine; E1, Putrescine; E2, Spermidine; E3, Spermine; E4, Pyridoxine; E5, Pyridoxal; E6, Pyridoxamine; E7, β-Alanine; E8, D-Pantothenic Acid; E9, Orotic Acid; E10, Uracil; E11, Uridine; E12, 2'-Deoxy Uridine; F1, Quinolinic Acid; F2, Nicotinic Acid; F3, Nicotinamide; F4, β-Nicotinamide Adenine Dinucleotide; F5, δ-Amino Levulinic Acid; F6, Hematin F7, Deferoxamine; Mesylate; F8, D-(+)-Glucose; F9, N-Acetyl D-Glucosamine; F10, Thymine; F11, Glutathione (reduced form); F12, Thymidine; G1, Oxaloacetic Acid; G2, D-Biotin; G3, CyanoCobalamine; G4, p-Amino Benzoic Acid; G5, Folic Acid; G6, Inosine +Thiamine; G7, Thiamine; G8, Thiamine Pyrophosphate; G9, Riboflavin; G10, Pyrrolo-Quinoline Quinone; G11, Menadione; G12, m-Inositol; H1, Butyric Acid; H2, D,L-α-Hydroxy Butyric Acid; H3, α-Keto Butyric Acid; H4, Caprylic Acid; H5, D,L- α-Lipoic Acid (oxidized form); H6, D,L-Mevalonic Acid; H7, D,L-Carnitine; H8, Choline; H9, Tween 20; H10, Tween 40; H11, Tween 60; H12, Tween 80.
PM6 – Peptide Nitrogen sources	A1, Negative Control; A2, Positive Control: L-Glutamine; A3, Ala-Ala; A4, Ala-Arg; A5, Ala-Asn; A6, Ala-Glu; A7, Ala-Gly; A8, Ala-His; A9, Ala-Leu; A10, Ala-Lys; A11, Ala-Phe; A12, Ala-Pro; B1, Ala-Ser; B2, Ala-Thr; B3, Ala-Trp; B4, Ala-Tyr; B5, Arg-Ala; B6, Arg-Arg; B7, Arg-Asp; B8, Arg-Gln; B9, ; rg-Glu; B10, Arg-Ile; B11, Arg-Leu; B12, Arg-Lys; C1, Arg-Met; C2, Arg-Phe; C3, Arg-Ser; C4, Arg-; rp; C5, Arg-Tyr; C6, Arg-Val; C7, Asn-Glu; C8, Asn-Val; C9, Asp-Asp; C10, Asp-Glu; C11, Asp-Leu; C12, Asp-Lys; D1, Asp-Phe; D2, Asp-Trp; D3, Asp-Val; D4, Cys-Gly; D5, Gln-Gln ;D6, Gln-Gly; D7, Glu-Asp; D8, Glu-Glu; D9, Glu-Gly; D10, Glu-Ser; D11, Glu-Trp; D12, Glu-Tyr; E1, Glu-Val; E2, Gly-Ala; E3, Gly-Arg; E4, Gly-Cys; E5, Gly-Gly; E6, Gly-His; E7, Gly-Leu; E8, Gly-Lys; E9, Gly-Met; E10, Gly-Phe; E11, Gly-Pro; E12, Gly-Ser; F1, Gly-Thr; F2, Gly-Trp; F3, Gly-Tyr; F4, Gly-Val; F5, His-Asp; F6, His-Gly; F7, His-Leu; F8, His-Lys; F9, His-Met; F10, His-Pro; F11 ,His-Ser; F12, His-Trp; G1, His-Tyr; G2, His-Val; G3, Ile-Ala; G4, Ile-Arg; G5, Ile-Gln; G6, Ile-Gly; G7, Ile-His; G8, Ile-Ile; G9, Ile-Met; G10, Ile-Phe; G11, Ile-Pro; G12, Ile-Ser; H1, Ile-Trp; H2, Ile-Tyr; H3, Ile-Val; H4, Leu-Ala; H5, Leu-Arg; H6, Leu-Asp; H7, Leu-Glu; H8, Leu-Gly; H9, Leu-Ile; H10, Leu-Leu; H11, Leu-Met; H12, Leu-Phe.
PM7 – Peptide Nitrogen sources	A1, Negative Control; A2, Positive Control: L-Glutamine; A3, Leu-Ser; A4, Leu-Trp; A5, Leu-Val; A6, Lys-Ala; A7, Lys-Arg; A8, Lys-Glu; A9, Lys-Ile; A10, Lys-Leu; A11, Lys-Lys; A12, Lys-Phe; B1, Lys-Pro; B2, Lys-Ser; B3, Lys-Thr; B4, Lys-Trp; B5 ,Lys-Tyr; B6, Lys-Val; B7, Met-Arg; B8, Met-Asp; B9, Met-Gln; B10, Met-Glu; B11, Met-Gly; B12, Met-His; C1, Met-Ile; C2, Met-Leu; C3, Met-Lys; C4, Met-Met; C5, Met-Phe; C6, Met-Pro; C7, Met-Trp; C8, Met-Val; C9, Phe-Ala; C10, Phe-Gly; C11, Phe-Ile; C12, Phe-Phe; D1, Phe-Pro; D2, Phe-Ser; D3, Phe-Trp; D4, Pro-Ala; D5, Pro-Asp; D6, Pro-Gln; D7, Pro-Gly; D8, Pro-Hyp; D9, Pro-Leu; D10, Pro-Phe; D11, Pro-Pro; D12, Pro-Tyr; E1, Ser-Ala; E2, Ser-Gly; E3, Ser-His; E4, Ser-Leu; E5, Ser-Met; E6, Ser-Phe; E7, Ser-Pro; E8, Ser-Ser; E9, Ser-Tyr; E10, Ser-Val; E11, Thr-Ala; E12, Thr-Arg; F1, Thr-Glu; F2, Thr-Gly; F3, Thr-Leu; F4, Thr-Met; F5, Thr-Pro; F6, Trp-Ala; F7, Trp-Arg; F8, Trp-Asp; F9, Trp-Glu; F10, Trp-Gly;

	F11, Trp-Leu; F12, Trp-Lys; G1, Trp-Phe; G2, Trp-Ser; G3, Trp-Trp; G4, Trp-Tyr; G5, Tyr-Ala; G6, Tyr-Gln; G7, Tyr-Glu; G8, Tyr-Gly G9, Tyr-His; G10, Tyr-Leu; G11, Tyr-Lys; G12, Tyr-Phe; H1, Tyr-Trp; H2, Tyr-Tyr; H3, Val-Arg; H4, Val-Asn; H5, Val-Asp; H6, Val-Gly; H7, Val-His; H8, Val-Ile; H9, Val-Leu; H10, Val-Tyr; H11, Val-Val; H12, Y-Glu-Gly.
PM8 – Peptide Nitrogen sources	A1, Negative Control; A2, Positive Control: L-Glutamine; A3, Ala-Asp; A4, Ala-Gln; A5, Ala-Ile; A6, Ala-Met; A7, Ala-Val; A8, Asp-Ala; A9, Asp-Gln; A10, Asp-Gly; A11, Glu-Ala; A12, Gly-Asn; B1, Gly-Asp; B2, Gly-Ile; B3, His-Ala; B4, His-Glu; B5, His-His; B6, Ile-Asn; B7, Ile-Leu; B8, Leu-Asn; B9, Leu-His; B10, Leu-Pro; B11, Leu-Tyr; B12, Lys-Asp; C1, Lys-Gly; C2, Lys-Met; C3, Met-Thr; C4, Met-Tyr; C5, Phe-Asp; C6, Phe-Glu; C7, Gln-Glu; C8, Phe-Met; C9, Phe-Tyr; C10, Phe-Val; C11, Pro-Arg; C12, Pro-Asn; D1, Pro-Glu; D2, Pro-Ile; D3, Pro-Lys; D4, Pro-Ser; D5, Pro-Trp; D6, Pro-Val; D7, Ser-Asn; D8, Ser-Asp; D9, Ser-Gln; D10, Ser-Glu; D11, Thr-Asp; D12, Thr-Gln; E1, Thr-Phe; E2, Thr-Ser; E3, Trp-Val; E4, Tyr-Ile; E5, Tyr-Val; E6, Val-Ala; E7, Val-Gln; E8, Val-Glu; E9, Val-Lys; E10, Val-Met; E11, Val-Phe; E12, Val-Pro; F1, Val-Ser; F2, β-Ala-Ala; F3, β-Ala-Gly; F4, β-Ala-His; F5, Met- β-Ala; F6, β-Ala-Phe; F7, D-Ala-D-Ala; F8, D-Ala-Gly; F9, D-Ala-Leu; F10, D-Leu-D-Leu; F11, D-Leu-Gly; F12, D-Leu-Tyr; G1, Y-Glu-Gly; G2, Y-D-Glu-Gly; G3, Gly-D-Ala; G4, Gly-D-Asp; G5, Gly-D-Ser; G6, Gly-D-Thr; G7, Gly-D-Val; G8, Leu-β-Ala; G9, Leu-D-Leu; G10, Phe-β-Ala; G11, Ala-Ala-Ala; G12, D-Ala-Gly-Gly; H1, Gly-Gly-Ala; H2, Gly-Gly-D-Leu; H3, Gly-Gly-Gly; H4, Gly-Gly-Ile; H5, Gly-Gly-Leu; H6, Gly-Gly-Phe; H7, Val-Tyr-Val; H8, Gly-Phe-Phe; H9, Leu-Gly-Gly; H10, Leu-Leu-Leu; H11, Phe-Gly-Gly; H12, Tyr-Gly-Gly.
PM9 – Osmolytes	A1, NaCl 1%; A2, NaCl 2%; A3, NaCl 3%; A4, NaCl 4%; A5, NaCl 5%; A6, NaCl 5.5%; A7, NaCl 6%; A8, NaCl 6.5%; A9, NaCl 7%; A10, NaCl 8%; A11, NaCl 9%; A12, NaCl 10%; B1, NaCl 6%; B2, NaCl 6% +Betaine; B3, NaCl 6% +N-N Dimethyl Glycine; B4, NaCl 6% + Sarcosine; B5, NaCl 6% + Dimethyl sulphonyl propionate; B6, NaCl 6% + MOPS; B7, NaCl 6% + Ectoine; B8, NaCl 6% + Choline; B9, NaCl 6% + Phosphoryl Choline; B10, NaCl 6% + Creatine; B11, NaCl 6% + Creatinine; B12, NaCl 6% + L-Carnitine; C1, NaCl 6% + KCl; C2, NaCl 6% + L-Proline; C3, NaCl 6% + N-Acetyl L-Glutamine; C4, NaC1 6% + β-Glutamic Acid; C5 ,NaC1 6% + γ–Amino –N Butyric Acid; C6, NaC1 6% + Glutathione; C7, NaCl 6% + Glycerol; C8, NaC1 6% +Trehalose; C9, NaC1 6% + TrimethylamineN-oxide; C10, NaC1 6% + Trimethylamine; C11, NaCl 6% + Octopine; C12, NaC1 6% + Trigonelline; D1, Potassium chloride 3%; D2, Potassium chloride 4%; D3, Potassium chloride 5%; D4, Potassium chloride 6%; D5, Sodium sulphate 2%; D6, Sodium sulphate 3%; D7, Sodium sulphate 4%; D8, Sodium sulphate 5%; D9, Ethylene glycol 5%; D10, Ethylene glycol 10%; D11, Ethylene glycol 15%; D12, Ethylene glycol 20%; E1, Sodium formate 1%; E2, Sodium formate 2%; E3, Sodium formate 3%; E4, Sodium formate 4%; E5, Sodium formate 5%; E6, Sodium formate 6%; E7, Urea 2%; E8, Urea 3%; E9, Urea 4%; E10, Urea 5%; E11, Urea 6%; E12, Urea 7%; F1, Sodium Lactate 1%; F2, Sodium Lactate 2%; F3, Sodium Lactate 3%; F4, Sodium Lactate 4%; F5, Sodium Lactate 5%; F6, Sodium Lactate 6%; F7, Sodium Lactate 7%; F8, Sodium Lactate 8%; F9, Sodium Lactate 9%; F10, Sodium Lactate 10%; F11, Sodium Lactate 11%; F12, Sodium Lactate 12%; G1, Sodium Phosphate pH 7 20mM; G2, Sodium Phosphate pH 7 50mM; G3, Sodium Phosphate pH 7 100mM; G4, Sodium Phosphate pH 7 200mM; G5, Sodium Benzoate pH 5.2 20mM; G6, Sodium Benzoate pH 5.2 50mM; G7, Sodium Benzoate pH5.2 100mM; G8, Sodium Benzoate pH 5.2 200mM; G9, Ammonium sulfate pH8 10mM; G10, Ammonium sulfate pH 8 20mM; G11, Ammonium sulfate pH 8 50mM; G12, Ammonium sulfate pH8 100mM; H1, Sodium Nitrate 10mM; H2, Sodium Nitrate 20mM; H3, Sodium Nitrate 40mM; H4, Sodium Nitrate 60mM; H5, Sodium Nitrate 80mM; H6, Sodium Nitrate 100mM; H7, Sodium Nitrite 10mM; H8, Sodium Nitrite 20mM; H9, Sodium Nitrite 40mM; H10, Sodium Nitrite 60mM; H11, Sodium Nitrite 80mM; H12, Sodium Nitrite 100mM.

PM10 – pH	A1, pH 3.5; A2, pH 4; A3, pH 4.5; A4, pH 5; A5, pH 5.5; A6, pH 6; A7, pH 7; A8, pH 8; A9, pH 8.5; A10, pH 9; A11, pH 9.5; A12, pH 10; B1, pH 4.5; B2, pH 4.5 + L-Alanine; B3, pH 4.5 + L-Arginine; B4, pH 4.5 + L-Asparagine; B5, pH 4.5 + L-Aspartic Acid; B6, pH 4.5 + L-Glutamic Acid; B7, pH 4.5 + L-Glutamine; B8, pH 4.5 + Glycine; B9, pH 4.5 + L-Histidine; B10, pH 4.5 + L-Isoleucine; B11, pH 4.5 + L-Leucine; B12, pH 4.5 + L-Lysine; C1, pH 4.5 + L-Methionine; C2, pH 4.5 + L-Phenylalanine; C3, pH 4.5 + L-Proline; C4, pH 4.5 + L-Serine; C5, pH 4.5 + L-Threonine; C6, pH 4.5 + L-Tryptophan; C7, pH 4.5 + L-Citrulline; C8, pH 4.5 + L-Valine; C9, pH 4.5 + HydroxyL-Proline; C10, pH 4.5 + L-Ornithine; C11, pH 4.5 + L-Homoarginine; C12, pH 4.5 + L-Homoserine; D-1, pH 4.5 + Anthranilic Acid; D2, pH 4.5 + L-Norleucine; D3, pH 4.5 + L-Norvaline; D4, pH 4.5 + α-Amino-N Butyric Acid; D5, pH 4.5 + p-Amino Benzoic Acid; D6, pH 4.5 + L-Cysteic Acid; D7, pH 4.5 + D-Lysine; D8, pH 4.5 + 5-Hydroxy Lysine; D9, pH 4.5 + 5-Hydroxy Tryptophan; D10, pH 4.5 + D,L-Diamino pimelic Acid; D11, pH 4.5 + Trimethylamine N-oxide; D12, pH 4.5 + Urea; E1, pH 9.5; E2, pH 9.5 + L-Alanine; E3, pH 9.5 + L-Arginine; E4, pH 9.5 + L-Asparagine; E5, pH 9.5 + L-Aspartic Acid; E6, pH 9.5 + L-Glutamic Acid; E7, pH 9.5 + L-Glutamine; E8, pH 9.5 + Glycine; E9, pH 9.5 + L-Histidine; E10, pH 9.5 + L-Isoleucine; E11, pH 9.5 + L-Leucine; E12, pH 9.5 + L-Lysine; F1, pH 9.5 + L-Methionine; F2, pH 9.5 + L-Phenylalanine; F3, pH 9.5 + L-Proline; F4, pH 9.5 + L-Serine; F5, pH 9.5 + L-Threonine; F6, pH 9.5 + L-Tryptophan; F7, pH 9.5 + L-Tyrosine; F8, pH 9.5 + L-Valine; F9, pH 9.5 + Hydroxy L-Proline; F10, pH 9.5 + L-Ornithine; F11, pH 9.5 + L-Homoarginine; F12, pH 9.5 + L-Homoserine; G1, pH 9.5 + Anthranilic acid; G2, pH 9.5 + L-Norleucine; G3, pH 9.5 + L-Norvaline; G4, pH 9.5 + Agmatine; G5, pH 9.5 + Cadaverine; G6, pH 9.5 + Putrescine; G7, pH 9.5 + Histamine; G8, pH 9.5 + Phenylethylamine; G9, pH 9.5 + Tyramine; G10, pH 9.5 + Creatine; G11, pH 9.5 + Trimethylamine N-oxide; G12, pH 9.5 + Urea; H1, X-Caprylate; H2, X–α-DGlucoside; H3, X-β-DGlucoside; H4, X-α-DGalactoside; H5, X-β-DGalactoside; H6, X-α- DGlucuronide; H7, X-β- DGlucuronide; H8, X-β-DGlucosaminide; H9, X-β-DGalactosaminide; H10, X-α-DMannoside; H11, X-PO4; H12, X-SO4.
PM11C – chemical	A1, Amikacin (1); A2, Amikacin (2); A3, Amikacin (3); A4, Amikacin (4); A5, Chlortetracycline (1); A6, Chlortetracycline (2) ;A7, Chlortetracycline (3); A8, Chlortetracycline (4); A9, Lincomycin (1); A10, Lincomycin (2); A11, Lincomycin (3); A12, Lincomycin (4); B1, Amoxicillin (1); B2, Amoxicillin (2); B3, Amoxicillin (3); B4, Amoxicillin (4); B5, Cloxacillin (1); B6, Cloxacillin (2); B7, Cloxacillin (3); B8, Cloxacillin (4); B9, Lomefloxacin (1); B10, Lomefloxacin (2); B11, Lomefloxacin (3); B12, Lomefloxacin (4); C1, Bleomycin (1); C2, Bleomycin (2); C3, Bleomycin (3); C4, Bleomycin (4); C5, Colistin (1); C6, Colistin (2); C7, Colistin (3); C8, Colistin (4); C9, Minocycline (1); C10, Minocycline (2); C11, Minocycline (3); C12, Minocycline (4); D1, Capreomycin (1); D2, Capreomycin (2); D3, Capreomycin (3); D4, Capreomycin (4); D5, Demeclocycline (1); D6, Demeclocycline (2); D7, Demeclocycline (3); D8, Demeclocycline (4); D9, Nafcillin (1); D10, Nafcillin (2); D11, Nafcillin (3); D12, Nafcillin (4); E1, Cefazolin (1); E2, Cefazolin (2); E3, Cefazolin (3); E4, Cefazolin (4); E5, Enoxacin (1); E6, Enoxacin (2); E7, Enoxacin (3); E8, Enoxacin (4); E9, Nalidixic acid (1); E10, Nalidixic acid (2); E11, Nalidixic acid (3); E12, Nalidixic acid (4); F1, Chloramphenicol (1); F2, Chloramphenicol (2); F3, Chloramphenicol (3); F4, Chloramphenicol (4); F5, Erythromycin (1); F6, Erythromycin (2); F7, Erythromycin (3); F8, Erythromycin (4); F9, Neomycin (1); F10, Neomycin (2); F11, Neomycin (3); F12, Neomycin (4); G1, Ceftriaxone (1); G2, Ceftriaxone (2); G3, Ceftriaxone (3); G4, Ceftriaxone (4); G5, Gentamicin (1); G6, Gentamicin (2); G7, Gentamicin (3); G8, Gentamicin (4); G9, Potassium tellurite (1); G10, Potassium tellurite (2); G11, Potassium tellurite (3); G12, Potassium tellurite (4); H1, Cephalothin (1); H2, Cephalothin (2); H3, Cephalothin (3); H4, Cephalothin (4); H5, Kanamycin (1); H6, Kanamycin (2); H7, Kanamycin (3); H8, Kanamycin (4); H9, Ofloxacin (1); H10, Ofloxacin

	(2); H11, Ofloxacin (3); H12, Ofloxacin (4).
PM12B – chemical	A1, Penicillin G (1); A2, Penicillin G (2); A3, Penicillin G (3); A4, Penicillin G (4); A5, Tetracycline (1); A6, Tetracycline (2); A7, Tetracycline (3); A8, Tetracycline (4); A9, Carbenicillin (1); A10, Carbenicillin (2); A11, Carbenicillin (3); A12, Carbenicillin (4); B1, Oxacillin (1); B2, Oxacillin (2); B3, Oxacillin (3); B4, Oxacillin (4); B5, Penimepicycline (1); B6, Penimepicycline (2); B7, Penimepicycline (3); B8, Penimepicycline (4); B9, Polymyxin B (1); B10, Polymyxin B (2); B11, Polymyxin B (3); B12, Polymyxin B (4); C1, Paromomycin (1); C2, Paromomycin (2); C3, Paromomycin (3); C4, Paromomycin (4); C5, Vancomycin (1); C6, Vancomycin (2); C7, Vancomycin (3); C8, Vancomycin (4); C9, D,L-Serinehydroxamate (1); C10, D,L-Serine hydroxamate (2); C11, D,L-Serine hydroxamate (3); C12, D,L-Serine hydroxamate (4); D1, Sisomicin (1); D2, Sisomicin (2); D3, Sisomicin (3); D4, Sisomicin (4); D5, Sulfamethazine (1); D6, Sulfamethazine (2); D7, Sulfamethazine (3); D8, Sulfamethazine (4); D9, Novobiocin (1); D10, Novobiocin (2); D11, Novobiocin (3); D12, Novobiocin (4); E1, 2,4-Diamino-6,7-diisopropylpteridine (1); E2, 2,4-Diamino-6,7-diisopropylpteridine (2); E3, 2,4-Diamino-6,7-diisopropylpteridine (3); E4, 2,4-Diamino-6,7-diisopropylpteridine (4); E5, Sulfadiazine (1); E6, Sulfadiazine (2); E7, Sulfadiazine (3); E8, Sulfadiazine (4); E9, Benzethoniumchloride (1); E10, Benzethoniumchloride (2); E11, Benzethoniumchloride (3); E12, Benzethoniumchloride (4); F1, Tobramycin (1); F2, Tobramycin (2); F3, Tobramycin (3); F4, Tobramycin (4); F5, Sulfathiazole (1); F6, Sulfathiazole (2); F7, Sulfathiazole (3); F8, Sulfathiazole (4); F9, 5-Fluoroorotic acid (1); F10, 5-Fluoroorotic acid (2); F11, 5-Fluoroorotic acid (3); F12, 5-Fluoroorotic acid (4); G1, Spectinomycin (1); G2, Spectinomycin (2); G3, Spectinomycin (3); G4, Spectinomycin (4); G5, Sulfamethoxazole (1); G6, Sulfamethoxazole (2); G7, Sulfamethoxazole (3); G8, Sulfamethoxazole (4); G9, L-Aspartic-β-hydroxamate (1); G10, L-Aspartic-β-hydroxamate (2); G11, L-Aspartic-β-hydroxamate (3); G12, L-Aspartic-β-hydroxamate (4); H1, Spiramycin (1); H2, Spiramycin (2); H3, Spiramycin (3); H4, Spiramycin (4); H5, Rifampicin (1); H6, Rifampicin (2); H7, Rifampicin (3); H8, Rifampicin (4); H9, Dodecyltrimethyl ammonium bromide (1); H10, Dodecyltrimethyl ammonium bromide (2); H11, Dodecyltrimethyl ammonium bromide (3); H12. Dodecyltrimethyl ammonium bromide (4).
PM13B – chemical	A1, Ampicillin (1); A2, Ampicillin (2); A3, Ampicillin (3); A4, Ampicillin (4); A5, Dequalinium chloride (1); A6, Dequalinium chloride (2); A7, Dequalinium chloride (3); A8, Dequalinium chloride (4); A9, Nickel chloride (1); A10, Nickel chloride (2); A11, Nickel chloride (3); A12, Nickel chloride (4); B1, Azlocillin (1); B2, Azlocillin (2); B3, Azlocillin (3); B4, Azlocillin (4); B5, 2, 2'-Dipyridyl (1); B6, 2, 2'-Dipyridyl (2); B7, 2, 2'-Dipyridyl (3); B8, 2, 2'-Dipyridyl (4); B9, Oxolinic acid (1); B10, Oxolinic acid (2); B11, Oxolinic acid (3); B12, Oxolinic acid (4); C1, 6-Mercaptopurine (1); C2, 6-Mercaptopurine (2); C3, -Mercaptopurine (3); C4, 6-Mercaptopurine (4); C5, Doxycycline (1); C6, Doxycycline (2); C7, Doxycycline (3); C8, Doxycycline (4); C9, Potassium chromate (1); C10, Potassium chromate (2); C11, Potassium chromate (3); C12, Potassium chromate (4); D1, Cefuroxime (1); D2, Cefuroxime (2); D3, Cefuroxime (3); D4, Cefuroxime (4); D5, 5-Fluorouracil (1); D6, 5-Fluorouracil (2); D7, 5-Fluorouracil (3); D8, 5-Fluorouracil (4); D9, Rolitetracycline (1); D10, Rolitetracycline (2); D11, Rolitetracycline (3); D12, Rolitetracycline (4); E1, Cytosine-1- βD-arabinofuranoside (1); E2, Cytosine-1- βD-arabinofuranoside (2); E3, Cytosine-1-βD-arabinofuranoside (3); E4, Cytosine-1-βD-arabinofuranoside (4); E5, Geneticin (G418) (1); E6, Geneticin (G418) (2); E7, Geneticin (G418) (3); E8, Geneticin (G418) (4); E9, Ruthenium red (1); E10, Ruthenium red (2); E11, Ruthenium red (3); E12, Ruthenium red (4); F1, Cesium chloride (1); F2, Cesium chloride (2); F3, Cesium chloride (3); F4, Cesium chloride (4); F5, Glycine (1); F6, Glycine (2); F7, Glycine (3); F8, Glycine (4); F9, Thallium (I) acetate (1); F10, Thallium (I) acetate (2); F11, Thallium (I) acetate (3); F12, Thallium (I) acetate (4); G1, Cobalt

	chloride (1); G2, Cobalt chloride (2); G3, Cobalt chloride (3); G4, Cobalt chloride (4); G5, Manganese chloride (1); G6, Manganese chloride (2); G7, Manganese chloride (3); G8, Manganese chloride (4); G9, Trifluoperazine (1); G10 ,Trifluoperazine (2); G11, Trifluoperazine (3); G12, Trifluoperazine (4); H1, Cupric chloride (1); H2, Cupric chloride (2); H3, Cupric chloride (3); H4, Cupric chloride (4); H5, Moxalactam (1); H6, Moxalactam (2); H7, Moxalactam (3); H8, Moxalactam (4); H9, Tylosin (1); H10, Tylosin (2); H11, Tylosin (3); H12, Tylosin (4).
PM14A – chemical	A1, Acriflavine (1); A2, Acriflavine (2); A3, Acriflavine (3); A4, Acriflavine (4); A5, Furaltadone (1); A6, Furaltadone (2); A7, Furaltadone (3); A8, Furaltadone (4); A9, Sanguinarine (1); A10, Sanguinarine (2); A11, Sanguinarine (3); A12, Sanguinarine (4); B1, 9-Aminoacridine (1); B2, 9-Aminoacridine (2); B3, 9-Aminoacridine (3); B4, 9-Aminoacridine (4); B5, Fusaric acid (1); B6, Fusaric acid (2); B7, Fusaric acid (3); B8, Fusaric acid (4); B9, Sodium arsenate (1); B10, Sodium arsenate (2); B11, Sodium arsenate (3); B12, Sodium arsenate (4); C1, Boric Acid (1); C2, Boric Acid (2); C3, Boric Acid (3); C4, Boric Acid (4); C5, 1-Hydroxypyridine-2-thione (1); C6, 1-Hydroxypyridine-2-thione (2); C7, 1-Hydroxypyridine-2-thione (3); C8, 1-Hydroxypyridine-2-thione (4); C9, Sodium cyanate (1); C10, Sodium cyanate (2); C11, Sodium cyanate (3); C12, Sodium cyanate (4); D1, Cadmium chloride (1); D2, Cadmium chloride (2); D3, Cadmium chloride (3); D4, Cadmium chloride (4); D5, Iodoacetate (1); D6, Iodoacetate (2); D7, Iodoacetate (3); D8, Iodoacetate (4); D9, Sodium dichromate (1); D10, Sodium dichromate (2); D11, Sodium dichromate (3); D12, Sodium dichromate (4); E1, Cefoxitin (1); E2, Cefoxitin (2); E3, Cefoxitin (3); E4, Cefoxitin (4); E5, Nitrofurantoin (1); E6, Nitrofurantoin (2); E7, Nitrofurantoin (3); E8, Nitrofurantoin (4); E9, Sodium metaborate (1); E10, Sodium metaborate (2); E11, Sodium metaborate (3); E12, Sodium metaborate (4); F1, Chloramphenicol (1); F2, Chloramphenicol (2); F3, Chloramphenicol (3); F4, Chloramphenicol (4); F5, Piperacillin (1); F6, Piperacillin (2); F7, Piperacillin (3); F8, Piperacillin (4); F9, Sodium metavanadate (1); F10, Sodium metavanadate (2); F11, Sodium metavanadate (3); F12, Sodium metavanadate (4); G1, Chelerythrine (1); G2, Chelerythrine (2); G3, Chelerythrine (3); G4, Chelerythrine (4); G5, Carbenicillin (1); G6, Carbenicillin (2); G7, Carbenicillin (3); G8, Carbenicillin (4); G9, Sodium nitrite (1); G10, Sodium nitrite (2); G11, Sodium nitrite (3); G12, Sodium nitrite (4); H1 ,EGTA (1); H2, EGTA (2); H3, EGTA (3); H4, EGTA (4); H5, Promethazine (1); H6, Promethazine (2); H7, Promethazine (3); H8, Promethazine (4); H9, Sodium orthovanadate (1); H10, Sodium orthovanadate (2); H11, Sodium orthovanadate (3); H12, Sodium orthovanadate (4).
PM15B – chemical	A1, Procaine (1) ;A2, Procaine (2); A3, Procaine (3); A4, Procaine (4); A5, Guanidine hydrochloride (1); A6, Guanidine hydrochloride (2); A7, Guanidine hydrochloride (3); A8, Guanidine hydrochloride (4); A9, Cefmetazole (1); A10, Cefmetazole (2); A11, Cefmetazole (3); A12, Cefmetazole (4); B1, D-Cycloserine (1); B2, D-Cycloserine (2); B3, D-Cycloserine (3); B4, D-Cycloserine (4); B5, EDTA (1); B6, EDTA (2); B7, EDTA (3); B8, EDTA (4); B9, 5,7-Dichloro- 8-hydroxyquinaldine (1); B10, 5,7-Dichloro- 8-hydroxyquinaldine (2); B11, 5,7-Dichloro- 8-hydroxyquinaldine (3); B12, 5,7-Dichloro- 8-hydroxyquinaldine (4); C1, 5,7-Dichloro-8-hydroxyquinoline (1); C2, 5,7-Dichloro-8-hydroxyquinoline (2); C3, 5,7-Dichloro-8-hydroxyquinoline (3); C4, 5,7-Dichloro-8-hydroxyquinoline (4); C5, Fusidic acid (1); C6, Fusidic acid (2); C7, Fusidic acid (3); C8, Fusidic acid (4); C9, 1,10-Phenanthroline (1); C10, 1,10-Phenanthroline (2); C11, 1,10-Phenanthroline (3); C12, 1,10-Phenanthroline (4); D1, Phleomycin (1); D2, Phleomycin (2); D3, Phleomycin (3); D4, Phleomycin (4); D5, Domiphen bromide (1); D6, Domiphen bromide (2); D7, Domiphen bromide (3); D8, Domiphen bromide (4); D9, Nordihydroguaia retic acid (1); D10, Nordihydroguaia retic acid (2); D11, Nordihydroguaia retic acid (3); D12, Nordihydroguaia retic acid (4); E1, Alexidine (1); E2, Alexidine (2); E3, Alexidine (3);

	E4, Alexidine (4); E5, 5-Nitro-2-furaldehyde semicarbazone (1); E6, 5-Nitro-2-furaldehyde semicarbazone (2); E7, 5-Nitro-2-furaldehyde semicarbazone (3); E8, 5-Nitro-2-furaldehyde semicarbazone (4); E9, Methyl viologen (1); E10, Methyl viologen (2); E11, Methyl viologen (3); E12, Methyl viologen (4); F1, 3, 4-Dimethoxybenzyl alcohol (1); F2, 3, 4-Dimethoxybenzyl alcohol (2); F3, 3, 4-Dimethoxybenzyl alcohol (3); F4, 3, 4-Dimethoxybenzyl alcohol (4); F5, Oleandomycin (1); F6, Oleandomycin (2); F7, Oleandomycin (3); F8, Oleandomycin (4); F9, Puromycin (1); F10, Puromycin (2); F11, Puromycin (3); F12, Puromycin (4); G1, CCCP (1); G2, CCCP (2); G3, CCCP (3); G4, CCCP (4); G5, Sodium azide (1); G6, Sodium azide (2); G7, Sodium azide (3); G8, Sodium azide (4); G9, Menadione (1); G10, Menadione (2); G11, Menadione (3); G12, Menadione (4); H1, 2-Nitroimidazole (1); H2, 2-Nitroimidazole (2); H3, 2-Nitroimidazole (3); H4, 2-Nitroimidazole (4); H5, Hydroxyurea (1); H6, Hydroxyurea (2); H7, Hydroxyurea (3); H8, Hydroxyurea (4); H9, Zinc chloride (1); H10, Zinc chloride (2); H11, Zinc chloride (3); H12, Zinc chloride (4).
PM16A – chemical	A1, Cefotaxime (1); A2, Cefotaxime (2); A3, Cefotaxime (3); A4, Cefotaxime (4); A5, Phosphomycin (1); A6, Phosphomycin (2); A7, Phosphomycin (3); A8, Phosphomycin (4); A9, 5-Chloro-7-iodo-8-hydroxyquinoline (1); A10, 5-Chloro-7-iodo-8-hydroxyquinoline (2); A11, 5-Chloro-7-iodo-8-hydroxyquinoline (3); A12, 5-Chloro-7-iodo-8-hydroxyquinoline (4); B1, Norfloxacin (1); B2, Norfloxacin (2); B3, Norfloxacin (3); B4, Norfloxacin (4); B5, Sulfanilamide (1); B6, Sulfanilamide (2); B7, Sulfanilamide (3); B8, Sulfanilamide (4); B9, Trimethoprim (1); B10, Trimethoprim (2); B11, Trimethoprim (3); B12, Trimethoprim (4); C1, Dichlofluanid (1); C2, Dichlofluanid (2); C3, Dichlofluanid (3); C4, Dichlofluanid (4); C5, Protamine sulfate (1); C6, Protamine sulfate (2); C7, Protamine sulfate (3); C8, Protamine sulfate (4); C9, Cetylpyridinium chloride (1); C10, Cetylpyridinium chloride (2); C11, Cetylpyridinium chloride (3); C12, Cetylpyridinium chloride (4); D1, 1-Chloro -2,4-dinitrobenzene (1); D2, 1-Chloro -2,4-dinitrobenzene (2); D3, 1-Chloro -2,4-dinitrobenzene (3); D4, 1-Chloro -2,4-dinitrobenzene (4); D5, Diamide (1); D6, Diamide (2); D7, Diamide (3); D8, Diamide (4); D9, Cinoxacin (1); D10, Cinoxacin (2); D11, Cinoxacin (3); D12, Cinoxacin (4); E1, Streptomycin (1); E2, Streptomycin (2); E3, Streptomycin (3); E4, Streptomycin (4); E5, 5-Azacytidine (1); E6, 5-Azacytidine (2); E7, 5-Azacytidine (3); E8, 5-Azacytidine (4); E9, Rifamycin SV (1); E10, Rifamycin SV (2); E11, Rifamycin SV (3); E12, Rifamycin SV (4); F1, Potassium tellurite (1); F2, Potassium tellurite (2); F3, Potassium tellurite (3); F4, Potassium tellurite (4); F5, Sodium selenite (1); F6, Sodium selenite (2); F7, Sodium selenite (3); F8, Sodium selenite (4); F9, Aluminum sulfate (1); F10, Aluminum sulfate (2); F11, Aluminum sulfate (3); F12, Aluminum sulfate (4); G1, Chromium chloride (1); G2, Chromium chloride (2); G3, Chromium chloride (3); G4, Chromium chloride (4); G5, Ferric chloride (1); G6, Ferric chloride (2); G7, Ferric chloride (3); G8, Ferric chloride (4); G9, L-Glutamic-ghydroxamate (1); G10, L-Glutamic-ghydroxamate (2); G11, L-Glutamic-ghydroxamate (3); G12, L-Glutamic-ghydroxamate (4); H1, Glycine hydroxamate (1); H2, Glycine hydroxamate (2); H3, Glycine hydroxamate (3); H4, Glycine hydroxamate (4); H5, Chloroxylenol (1); H6, Chloroxylenol (2); H7, Chloroxylenol (3); H8, Chloroxylenol (4); H9, Sorbic acid (1); H10, Sorbic acid (2); H11, Sorbic acid (3); H12, Sorbic acid (4).
PM17A – chemical	A1, D-Serine (1); A2, D-Serine (2); A3, D-Serine (3); A4, D-Serine (4); A5, β-ChloroL-alanine hydrochloride (1); A6, β-ChloroL-alanine hydrochloride (2); A7, β-ChloroL-alanine hydrochloride (3); A8, β-ChloroL-alanine hydrochloride (4); A9, Thiosalicylic acid (1); A10, Thiosalicylic acid (2); A11, Thiosalicylic acid (3); A12, Thiosalicylic acid (4); B1, Sodium salicylate (1); B2, Sodium salicylate (2); B3, Sodium salicylate (3); B4, Sodium salicylate (4); B5, Hygromycin B (1); B6, Hygromycin B (2); B7, Hygromycin B (3); B8, Hygromycin B (4); B9, Ethionamide (1); B10, Ethionamide (2); B11, Ethionamide (3); B12, Ethionamide (4); C1, 4-Aminopyridine (1); C2, 4-Aminopyridine (2); C3, 4-Aminopyridine

	(3); C4, 4-Aminopyridine (4); C5, Sulfachloropyridazine (1); C6, Sulfachloropyridazine (2); C7, Sulfachloropyridazine (3); C8, Sulfachloropyridazine (4); C9, Sulfamonomethoxine (1); C10, Sulfamonomethoxine (2); C11, Sulfamonomethoxine (3); C12, Sulfamonomethoxine (4); D1, Oxycarboxin (1); D2, Oxycarboxin (2); D3, Oxycarboxin (3); D4, Oxycarboxin (4); D5, 3-Amino-1,2,4-triazole (1); D6, 3-Amino-1,2,4-triazole (2); D7, 3-Amino-1,2,4-triazole (3); D8, 3-Amino-1,2,4-triazole (4); D9, Chlorpromazine (1); D10, Chlorpromazine (2); D11, Chlorpromazine (3); D12, Chlorpromazine (4); E1, Niaproof (1); E2, Niaproof (2); E3, Niaproof (3); E4, Niaproof (4); E5, Compound 48/80 (1); E6, Compound 48/80 (2); E7, Compound 48/80 (3); E8, Compound 48/80 (4); E9, Sodium tungstate (1); E10, Sodium tungstate (2); E11, Sodium tungstate (3); E12, Sodium tungstate (4); F1, Lithium chloride (1); F2, Lithium chloride (2) F3, Lithium chloride (3); F4, Lithium chloride (4); F5, DL-Methionine hydroxamate (1); F6, DL-Methionine hydroxamate (2); F7, DL-Methionine hydroxamate (3); F8, DL-Methionine hydroxamate (4); F9, Tannic acid (1); F10, Tannic acid (2); F11, Tannic acid (3); F12, Tannic acid (4); G1, Chlorambucil (1); G2, Chlorambucil (2); G3, Chlorambucil (3); G4, Chlorambucil (4); G5, Cefamandole nafate (1); G6, Cefamandole nafate (2); G7, Cefamandole nafate (3); G8, Cefamandole nafate (4); G9, Cefoperazone (1); G10, Cefoperazone (2); G11, Cefoperazone (3); G12, Cefoperazone (4); H1, Cefsulodin (1); H2, Cefsulodin (2); H3, Cefsulodin (3); H4, Cefsulodin (4); H5, Caffeine (1); H6, Caffeine (2); H7, Caffeine (3); H8, Caffeine (4); H9, Phenylarsine oxide (1); H10, Phenylarsine oxide (2); H11, Phenylarsine oxide (3); H12, Phenylarsine oxide (4).
PM18C – chemical	A1, Ketoprofen (1); A2, Ketoprofen (2); A3, Ketoprofen (3); A4, Ketoprofen (4); A5, Sodium pyrophosphate decahydrate (1); A6, Sodium pyrophosphate decahydrate (2); A7, Sodium pyrophosphate decahydrate (3); A8, Sodium pyrophosphate decahydrate (4); A9, Thiamphenicol (1); A10, Thiamphenicol (2); A11, Thiamphenicol (3); A12, Thiamphenicol (4); B1, Trifluorothymidine (1); B2, Trifluorothymidine (2); B3, Trifluorothymidine (3); B4, Trifluorothymidine (4); B5, Pipemidic Acid (1); B6, Pipemidic Acid (2); B7, Pipemidic Acid (3); B8, Pipemidic Acid (4); B9, Azathioprine (1); B10, Azathioprine (2); B11, Azathioprine (3); B12, Azathioprine (4); C1, Poly-L-lysine (1); C2, Poly-L-lysine (2); C3, Poly-L-lysine (3); C4, Poly-L-lysine (4); C5, Sulfisoxazole (1); C6, Sulfisoxazole (2); C7, Sulfisoxazole (3); C8, Sulfisoxazole (4); C9, Pentachlorophenol (1); C10, Pentachlorophenol (2); C11, Pentachlorophenol (3); C12, Pentachlorophenol (4); D1, Sodium m-arsenite (1); D2, Sodium m-arsenite (2); D3, Sodium m-arsenite (3); D4, Sodium m-arsenite (4); D5, Sodium bromate (1); D6, Sodium bromate (2); D7, Sodium bromate (3); D8, Sodium bromate (4); D9, Lidocaine (1); D10, Lidocaine (2); D11, Lidocaine (3); D12, Lidocaine (4); E1, Sodium metasilicate (1); E2, Sodium metasilicate (2); E3, Sodium metasilicate (3); E4, Sodium metasilicate (4); E5, Sodium m-periodate (1); E6, Sodium m-periodate (2); E7, Sodium m-periodate (3); E8, Sodium m-periodate (4); E9, Antimony (III) chloride (1); E10, Antimony (III) chloride (2); E11, Antimony (III) chloride (3); E12, Antimony (III) chloride (4); F1, Semicarbazide (1); F2, Semicarbazide (2); F3, Semicarbazide (3); F4, Semicarbazide (4); F5, Tinidazole (1); F6, Tinidazole (2); F7, Tinidazole (3); F8, Tinidazole (4); F9, Aztreonam (1); F10, Aztreonam (2); F11, Aztreonam (3); F12, Aztreonam (4); G1, Triclosan (1); G2, Triclosan (2); G3, Triclosan (3); G4, Triclosan (4); G5, 3,5-Diamino-1,2,4-triazole (Guanazole) (1); G6, 3,5-Diamino-1,2,4-triazole (Guanazole) (2); G7, 3,5-Diamino-1,2,4-triazole (Guanazole) (3); G8, 3,5-Diamino-1,2,4-triazole (Guanazole) (4); G9, Myricetin (1); G10, Myricetin (2); G11, Myricetin (3); G12, Myricetin (4); H1, 5-fluoro-5'-deoxyuridine (1); H2, 5-fluoro-5'-deoxyuridine (2); H3, 5-fluoro-5'-deoxyuridine (3); H4, 5-fluoro-5'-deoxyuridine (4); H5, 2-Phenylphenol (1); H6, 2-Phenylphenol (2); H7, 2-Phenylphenol (3); H8, 2-Phenylphenol (4); H9, Plumbagin (1); H10, Plumbagin (2); H11, Plumbagin (3); H12, Plumbagin (4).
PM19 – chemical	A1, Josamycin (1); A2, Josamycin (2); A3, Josamycin (3); A4, Josamycin (4); A5, Gallic

	acid (1); A6, Gallic acid (2); A7, Gallic acid (3); A8, Gallic acid (4); A9, Coumarin (1); A10, Coumarin (2); A11, Coumarin (3); A12, Coumarin (4); B1, Methyltrioctylammonium chloride (1); B2, Methyltrioctylammonium chloride (2); B3, Methyltrioctylammonium chloride (3); B4, Methyltrioctylammonium chloride (4); B5, Harmane (1); B6, Harmane (2); B7, Harmane (3); B8, Harmane (4); B9, 2,4-Dintrophenol (1); B10, 2,4-Dintrophenol (2); B11, 2,4-Dintrophenol (3); B12, 2,4-Dintrophenol (4); C1, Chlorhexidine (1); C2, Chlorhexidine (2); C3, Chlorhexidine (3); C4, Chlorhexidine (4); C5, Umbelliferone (1); C6, Umbelliferone (2); C7, Umbelliferone (3); C8, Umbelliferone (4); C9, Cinnamic acid (1); C10, Cinnamic acid (2); C11, Cinnamic acid (3); C12, Cinnamic acid (4); D1, Disulphiram (1); D2, Disulphiram (2); D3, Disulphiram (3); D4, Disulphiram (4); D5, Iodonitro Tetrazolium Violet (1); D6, Iodonitro Tetrazolium Violet (2); D7, Iodonitro Tetrazolium Violet (3); D8, Iodonitro Tetrazolium Violet (4); D9, Phenyl-methylsulfonylfluoride (PMSF) (1); D10, Phenyl- methylsulfonylfluoride (PMSF) (2); D11, Phenyl- methylsulfonylfluoride (PMSF) (3); D12, Phenyl- methylsulfonylfluoride (PMSF) (4); E1, FCCP (1); E2, FCCP (2); E3, FCCP (3); E4, FCCP (4); E5, D,L-Thioctic Acid (1); E6, D,L-Thioctic Acid (2); E7, D,L-Thioctic Acid (3); E8, D,L-Thioctic Acid (4); E9, Lawsone (1); E10, Lawsone (2); E11, Lawsone (3); E12, Lawsone (4); F1, Phenethicillin (1); F2, Phenethicillin (2); F3, Phenethicillin (3); F4, Phenethicillin (4); F5, Blasticidin S (1); F6, Blasticidin S (2); F7, Blasticidin S (3); F8, Blasticidin S (4); F9, Sodium caprylate (1); F10, Sodium caprylate (2); F11, Sodium caprylate (3); F12, Sodium caprylate (4); G1, Lauryl sulfobetaine (1); G2, Lauryl sulfobetaine (2); G3, Lauryl sulfobetaine (3); G4, Lauryl sulfobetaine (4); G5, Dihydrostreptomycin (1); G6, Dihydrostreptomycin (2); G7, Dihydrostreptomycin (3); G8, Dihydrostreptomycin (4); G9, Hydroxylamine (1); G10, Hydroxylamine (2); G11, Hydroxylamine (3); G12, Hydroxylamine (4); H1, Hexammine cobalt (III) chloride (1); H2, Hexammine cobalt (III) chloride (2); H3, Hexammine cobalt (III) chloride (3); H4, Hexammine cobalt (III) chloride (4); H5, Thioglycerol (1); H6, Thioglycerol (2); H7, Thioglycerol (3); H8, Thioglycerol (4); H9, Polymyxin B (1); H10, Polymyxin B (2); H11, Polymyxin B (3); H12, Polymyxin B (4).
PM20B – chemical	A1, Amitriptyline (1); A2, Amitriptyline (2); A3, Amitriptyline (3) A4, Amitriptyline (4); A5, Apramycin (1); A6, Apramycin(2); A7, Apramycin (3); A8, Apramycin (4); A9, Benserazide (1); A10, Benserazide (2); A11, Benserazide (3); A12, Benserazide (4); B1, Orphenadrine (1); B2, Orphenadrine (2); B3, Orphenadrine (3); B4, Orphenadrine (4); B5, D,L-Propranolol (1); B6, D,L-Propranolol (2); B7, D,L-Propranolol (3), B8, D,L-Propranolol (4); B9, Tetrazolium Violet (1); B10, Tetrazolium Violet (2); B11, Tetrazolium Violet (3); B12, Tetrazolium Violet (4); C1, Thioridazine (1); C2, Thioridazine (2); C3, Thioridazine (3); C4, Thioridazine (4); C5, Atropine (1); C6, Atropine (2); C7, Atropine (3); C8, Atropine (4); C9, Ornidazole (1); C10, Ornidazole (2); C11, Ornidazole (3); C12, Ornidazole (4); D1, Proflavine (1); D2, Proflavine (2); D3, Proflavine (3); D4, Proflavine (4); D5, Ciprofloxacin (1); D6, Ciprofloxacin (2); D7, Ciprofloxacin (3); D8, Ciprofloxacin (4); D9, 18-Crown-6 Ether (1); D10, 18-Crown-6 Ether (2); D11, 18-Crown-6 Ether (3); D12, 18-Crown-6 Ether (4); E1, Crystal violet (1); E2, Crystal violet (2); E3, Crystal violet (3); E4, Crystal violet (4); E5, Dodine (1); E6, Dodine (2); E7, Dodine (3); E8, Dodine (4); E9, Hexachlorophene (1); E10, Hexachlorophene (2); E11, Hexachlorophene (3); E12, Hexachlorophene (4); F1, 4-Hydroxycoumarin (1); F2, 4-Hydroxycoumarin (2); F3, 4-Hydroxycoumarin (3); F4, 4-Hydroxycoumarin (4); F5, Oxytetracycline (1); F6, Oxytetracycline (2); F7, Oxytetracycline (3); F8, Oxytetracycline (4); F9, Pridinol (1); F10, Pridinol (2); F11, Pridinol (3); F12, Pridinol (4); G1, Captan (1); G2, Captan (2); G3, Captan (3); G4, Captan (4); G5, 3,5-Dinitrobenzene (1); G6, 3,5-Dinitrobenzene (2); G7, 3,5-Dinitrobenzene (3); G8, 3,5-Dinitrobenzene (4); G9, 8-Hydroxyquinoline (1); G10, 8-Hydroxyquinoline (2); G11, 8-Hydroxyquinoline (3); G12, 8-Hydroxyquinoline (4); H1, Patulin (1); H2, Patulin (2); H3, Patulin (3); H4, Patulin (4); H5, Tolylfluanid (1); H6,

	Tolylfluanid (2); H7, Tolylfluanid (3); H8, Tolylfluanid (4); H9, Troleandomycin (1); H10, Troleandomycin (2); H11, Troleandomycin (3); H12, Troleandomycin (4).

723

724 **Supplementary Table 2. Genes missing from pCROD1 of *C. rodentium* ICC180**

725

Gene	Location	Function
ROD_RS25055	240..494	Replication regulatory protein repA2
ROD_RS25060	797..1654	Replication protein
ROD_RS25065	2593..3246	Hypothetical protein
ROD_RS25070	3339..3596	Antitoxin
ROD_RS25075	3598..3930	Hypothetical protein
ROD_RS25080	4318..4614	Transposase
ROD_RS25085	5726..6955	Autotransporter strand-loop-strand
ROD_RS25090	6939..11720	Autotransporter
ROD_RS25095	12358..12558	Hypothetical protein
ROD_RS25100	12814..13043	Transposase
ROD_RS25105	14045..14563	Fimbrial protein
ROD_RS25110	14636..17053	Fimbrial protein
ROD_RS25115	17046..17738	Fimbrial protein
ROD_RS25120	18251..18820	Hypothetical protein
ROD_RS25125	18945..19904	Hypothetical protein
ROD_RS25130	20068..20844	EAL domain-containing protein
ROD_RS25135	22328..26254	Autotransporter
ROD_RS25140	26743..26993	Toxin HigB-2
ROD_RS25145	27079..27339	Transcriptional regulator
ROD_RS25150	27957..30536	Usher protein
ROD_RS25155	30578..31048	Hypothetical protein
ROD_RS25160	33519..33941	Twitching motility protein PilT

ROD_RS25165	33938..34168	Virulence factor
ROD_RS25170	34837..35055	Hypothetical protein
ROD_RS25175	35057..35362	Hypothetical protein
ROD_RS25180	35364..35690	Hypothetical protein
ROD_RS25185	35680..36471	Resolvase
ROD_RS25190	36627..40730	Autotransporter
ROD_RS25730	41808..43358	Hypothetical protein
ROD_RS25205	43907..44329	Entry exclusion protein 2
ROD_RS25210	44567..45523	Hypothetical protein
ROD_RS25215	45875..46504	Serine recombinase
ROD_RS25220	46779..47306	Putative resolvase
ROD_RS25225	47600..48241	Chromosome partitioning protein ParA
ROD_RS25230	48333..48665	Molecular chaperone GroEL
ROD_RS25235	49280..50002	DNA repair protein
ROD_RS25240	50082..51653	Transposase
ROD_RS25250	52020..52697	Transposase
ROD_RS25255	52721..52750	Endonuclease
ROD_RS25260	53458..54144	Hypothetical protein
ROD_RS25265	54141..54449	Hypothetical protein

726

727

1

Figure 1. Whole genome sequencing shows that the *lux* operon and kanamcyin resistance gene have inserted at position 5,212,273 in the chromosome of *C. rodentium* ICC180, disrupting a putative site-specific DNA recombinase.

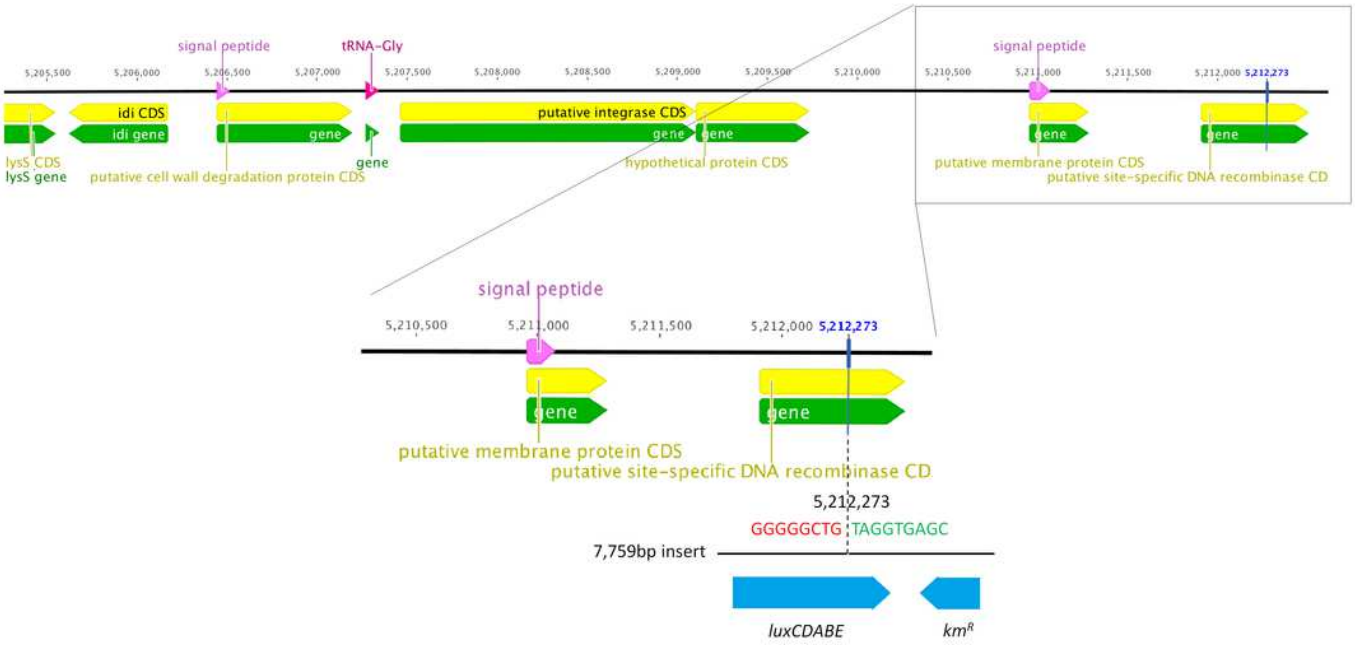

2

Figure 2. The growth of *Citrobacter rodentium* ICC180 compared to its non-bioluminescent parent strain ICC169 as assessed by phenotypic microarray (PM).

Wildtype *C. rodentium* ICC169 and its bioluminescent derivative ICC180 were grown on two separate occasions using PM plates 1-20. Activity rings from the PM data are shown where the grey inner circles indicate the strains' order and the external circle indicates the PM categories (see Key). The activity index (AV) was calculated for each strain in response to each well and the values for ICC169 are shown as colour stripes going from red (AV = 0 [not active]) to green (AV = 6 [active]; 7 total k-means clusters.

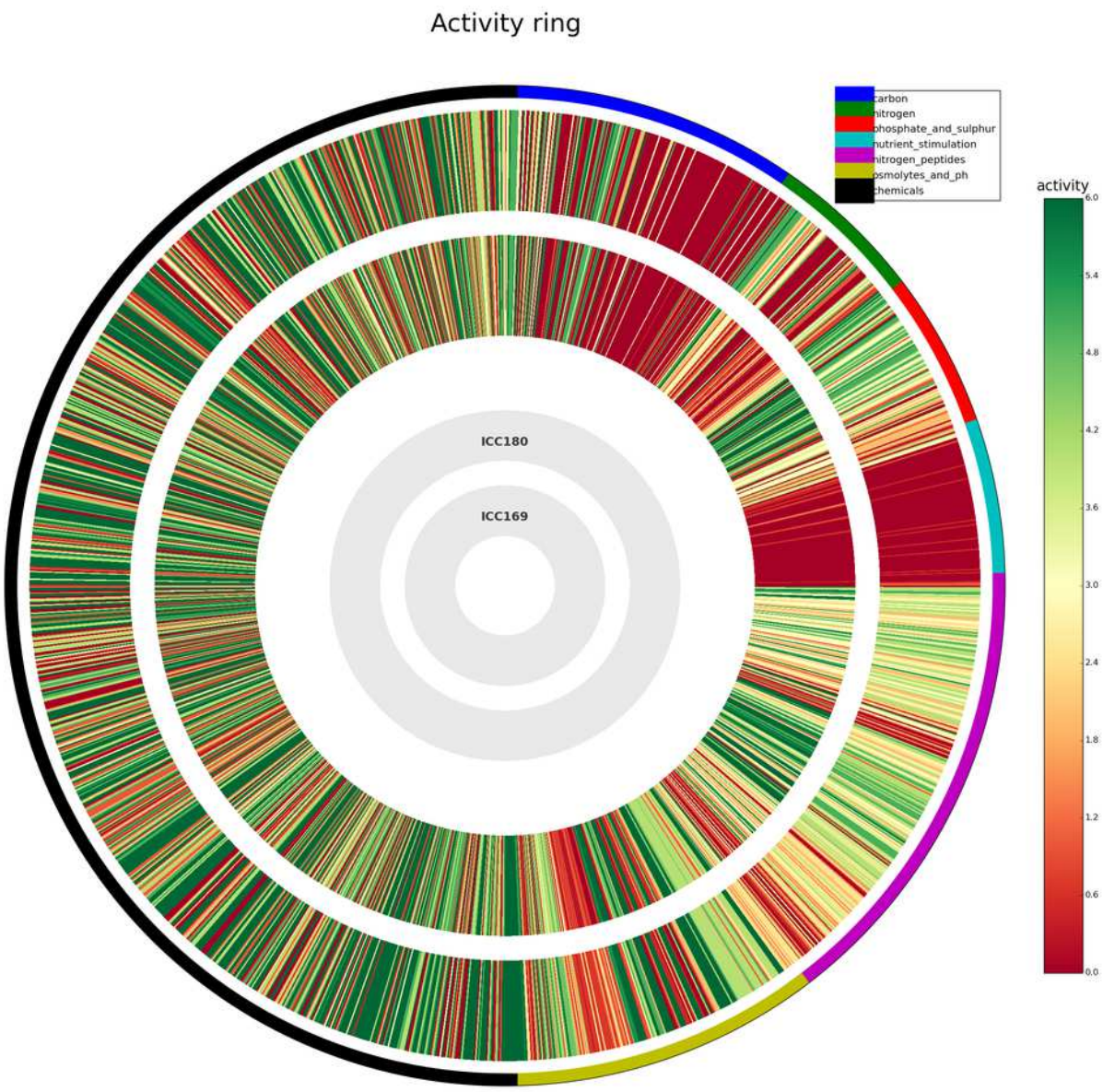

3

Figure 3. *C. rodentium* ICC180 is not impaired during growth in rich laboratory media when compared to its non-bioluminescent parent strain ICC169.

Wildtype *C. rodentium* ICC169 (shown as purple circles) and its bioluminescent derivative ICC180 (shown as blue triangles) were grown in LB-Lennox broth and monitored for changes in bioluminescence (given as relative light units [RLU] ml^{-1}) (A) and bacterial counts (given as colony forming units [CFU] ml^{-1}) (B). Bacterial count data was used to calculate Area Under Curve values for each strain (C). Data (medians with ranges where appropriate) is presented from experiments performed on eight separate occasions.

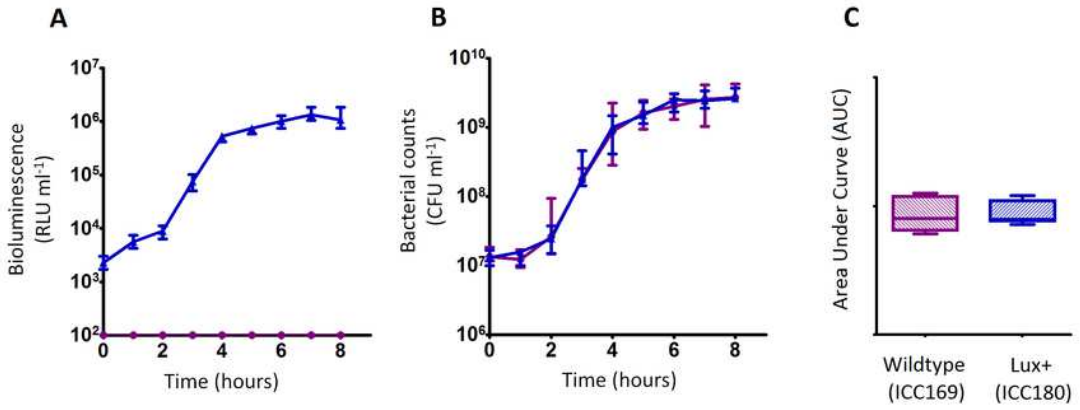

4

Figure 4. *C. rodentium* ICC180 is mildly impaired during growth in a defined minimal laboratory media when compared to its non-bioluminescent parent strain ICC169.

Wildtype *C. rodentium* ICC169 (shown as purple circles) and its bioluminescent derivative ICC180 (shown as blue triangles) were grown in minimal A salts supplemented with 1% glucose and monitored for changes in bioluminescence (given as relative light units [RLU] ml^{-1}) (A) and bacterial counts (given as colony forming units [CFU] ml^{-1}) (B). Bacterial count data was used to calculate Area Under Curve values for each strain, which were found to be significantly different (p=0.0078; Wilcoxon Matched pairs-signed rank test) (C). Data (medians with ranges where appropriate) is presented from experiments performed on eight separate occasions.

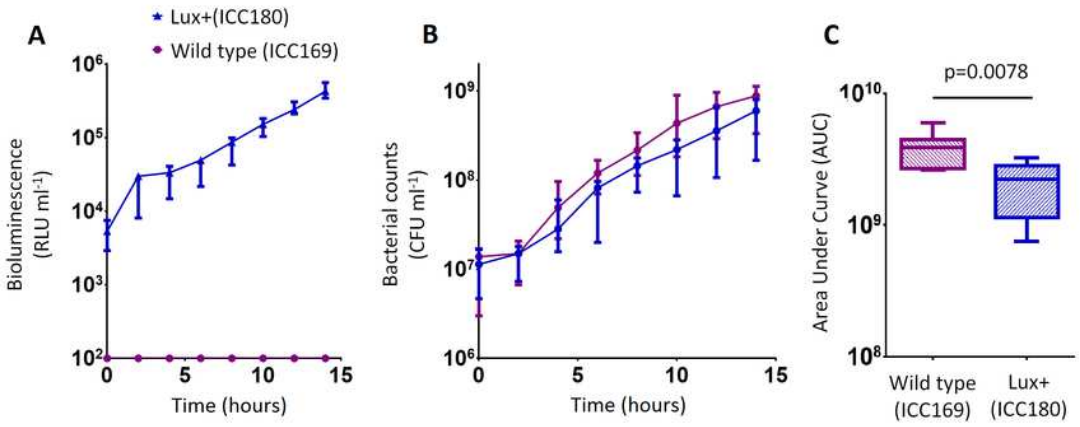

5

Figure 5. Bioluminescent *C. rodentium* ICC180 is not impaired in the *Galleria mellonella* infection model.

Groups of larvae (n = 10) of the Greater Wax Moth *Galleria mellonella* were infected with ICC169 and ICC180 in single and 1:1 mixed infections and monitored for survival (%) (A) and for disease symptoms using the Caterpillar Health Index (CHI), a numerical scoring system which measures degree of melanisation, silk production, motility, and mortality (given as median CHI values) (B). Survival curves (A) and calculated Area Under Curve data of CHI scores reveals no difference between waxworm response to infection from either strain (C). Waxworms infected with a 1:1 mix of ICC169 and ICC180 were homogenised at 24-hours, or at time of death if earlier. Actual infecting doses for each strain were determined by retrospective plating, and are indicated by *.The bacterial burden of ICC180 and ICC169 in individual caterpillars (indicated by the dotted line), was calculated after plating onto differential media and found to be significantly different (p=0.001; one-tailed Wilcoxon matched pairs-signed rank test) (D). Data (medians with ranges where appropriate) is presented from experiments performed on 3 separate occasions, except (A) and (D), where the results of a representative experiment are shown.

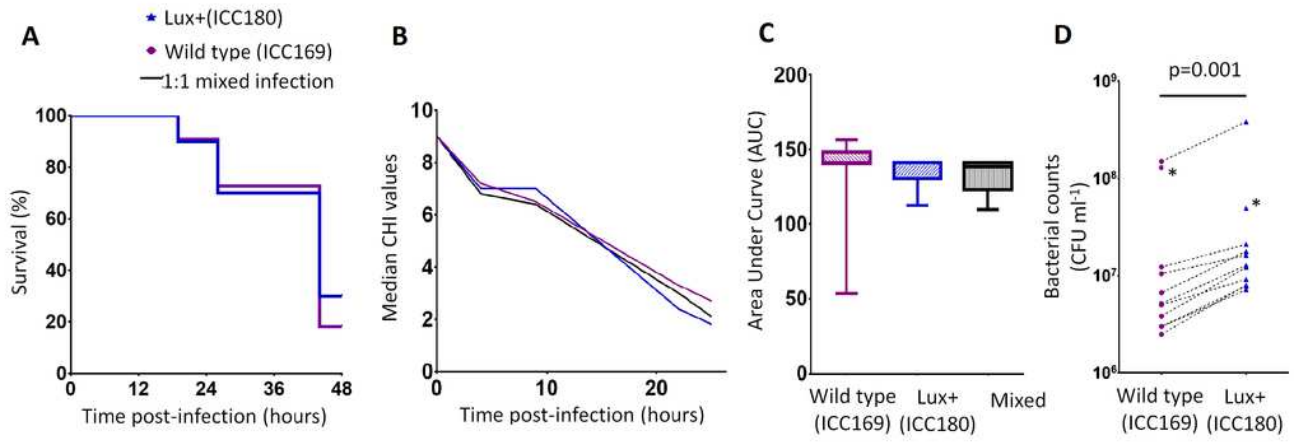

6

Figure 6. *C. rodentium* ICC180 is impaired during mixed, but not in single, infections in mice when compared to its non-bioluminescent parent strain ICC169.

Groups of female 6-8 week old C57Bl/6 mice (n=6) were orally-gavaged with ~5 x 10^9 CFU of wildtype *C. rodentium* ICC169 (shown as purple circles) and its bioluminescent derivative ICC180 (shown as blue triangles) in single infections (A, B) or 1:1 mixed infections (C, D) and monitored for changes in bacterial counts (given as colony forming units [CFU] g^{-1} stool) (A, B). Bacterial count data was used to calculate Area Under Curve values for each strain in single (B) and mixed (D) infections, and were found to be significantly different only for the mixed infections (p=0.001; one-tailed Wilcoxon Matched pairs-signed rank test). This is reflected in the competitive indices (CI) calculated from the bacterial counts recovered during mixed infections, with ICC180 showing a growing competitive disadvantage from day 2 post-infection (E). Data (medians with ranges where appropriate) is presented from experiments performed on two separate occasions.

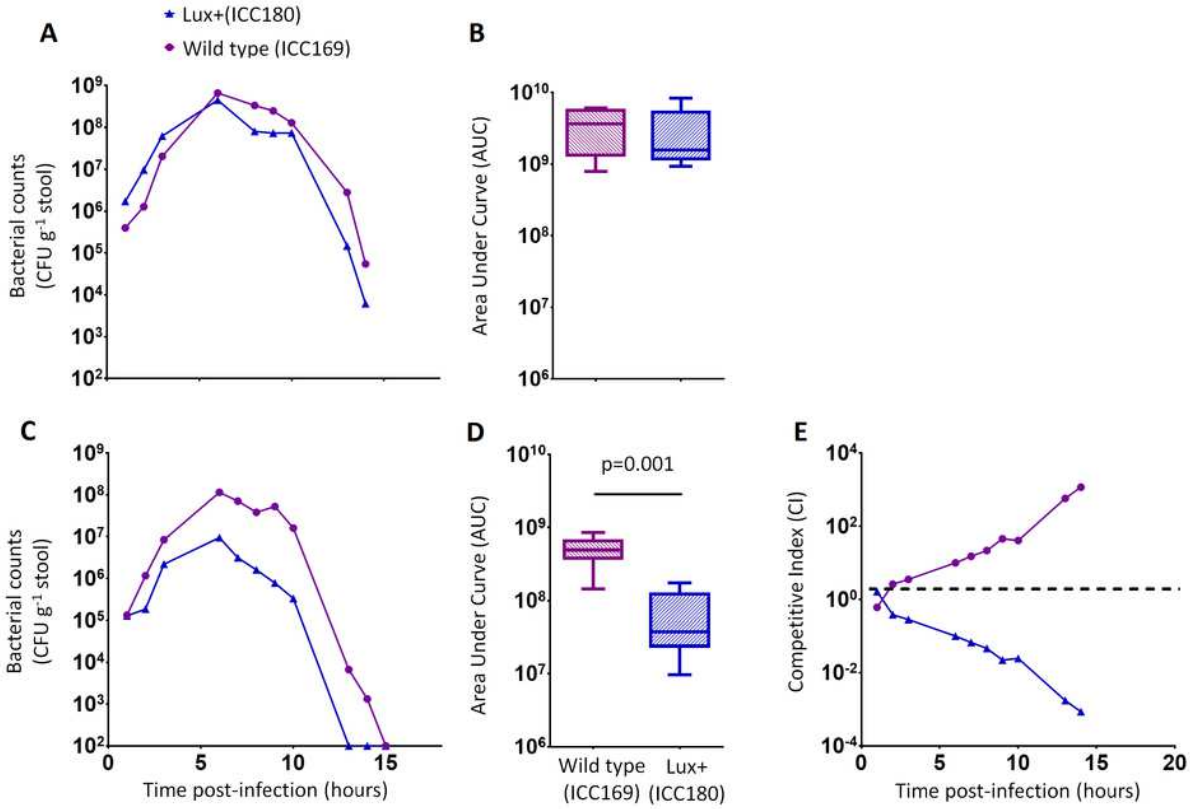

7

Figure 7. Despite having a fitness disadvantage in mixed infections of mice, ICC180 is still visible by biophotonic imaging.

Groups of female 6-8 week old C57Bl/6 mice (n=6) were orally-gavaged with ~5 x 10^9 CFU of wildtype *C. rodentium* ICC169 and its bioluminescent derivative ICC180 in single infections or 1:1 mixed infections. Bioluminescence (given as photons $second^{-1}$ cm^{-2} sr^{-1}) from ICC180 was measured after gaseous anesthesia with isoflurane using the IVIS® Kinetic camera system (Perkin Elmer). A photograph (reference image) was taken under low illumination before quantification of photons emitted from ICC180 at a binning of four over 1 minute using the Living Image software (Perkin Elmer). The sample shelf was set to position D (field of view, 12.5 cm). The images show peak bioluminescence with variations in colour representing light intensity at a given location and superimposed over the grey-scale reference image (A). Red represents the most intense light emission, whereas blue corresponds to the weakest signal. The color bar indicates relative signal intensity (as photons/second/cm^2/steradian [Sr]). Bioluminescence from the abdominal region of individual mice also was quantified using the region of interest tool in the Living Image software program (given as photons $second^{-1}$) and used to calculate Area Under Curve values for each individual animal (B). Dotted line represents background. Experiments were performed on two separate occasions. Three representative animals are shown.